

1 **Emission of volatile halogenated organic compounds**
2 **over various Dead Sea landscapes**
3
4
5
6
7
8

9 Moshe Shechner¹, Alex Guenther², Robert Rhew³, Asher Wishkerman⁴, Qian Li¹, Donald Blake², Gil Lerner¹ and
10 Eran Tas^{1*}
11

12 ¹The Robert H. Smith Faculty of Agriculture, Food and Environment, Department of Soil and Water Sciences, The
13 Hebrew University of Jerusalem, Rehovot, Israel

14 ²Department of Earth System Science, University of California, Irvine, CA, USA; Department of Geography at
15 Berkeley

16 ³ Department of Geography and Berkeley Atmospheric Sciences Center, University of California, Berkeley,
17 Berkeley, CA 94720, United States

18 ⁴Ruppin Academic Center, Michmoret, Israel; Department of Chemistry, University of California, Irvine, Irvine,
19 CA 92697
20
21
22
23
24
25
26

27 * Corresponding author – Eran Tas, The Department of Soil and Water Sciences, The Robert H.
28 Smith Faculty of Agriculture, Food and Environment, Hebrew University of Jerusalem,
29 Rehovot, Israel. eran.tas@mail.huji.ac.il
30
31
32

33 **Abstract.** Volatile halogenated organic compounds (VHOCs), such as methyl halides (CH_3X ; X
34 = Br, Cl and I) and very short-lived halogenated substances [VSLs; bromoform (CHBr_3),
35 dibromomethane (CH_2Br_2), bromodichloromethane (CHBrCl_2), trichloroethylene (C_2HCl_3),
36 chloroform (CHCl_3) and dibromochloromethane (CHBr_2Cl)] are well known for their significant
37 influence on ozone concentrations and oxidation capacity of the troposphere and stratosphere,
38 and for their key role in aerosol formation. Insufficient characterization of the sources and
39 emission rate of VHOCs limits our ability to understand and assess their impact in both the
40 troposphere and stratosphere. Over the last two decades, several natural terrestrial sources for
41 VHOCs, including soil and vegetation, have been identified, but our knowledge of emission
42 rates from these sources and their responses to changes in ambient conditions remains limited.
43 Here we report measurements of the mixing ratios and fluxes of several chlorinated and
44 brominated VHOCs from different landscapes and natural and agricultural vegetated sites at the
45 Dead Sea during different seasons. Fluxes were generally positive (emission into the
46 atmosphere), corresponding to elevated mixing ratios, but were highly variable. Fluxes (and
47 mixing ratios) for the investigated VHOCs ranged as follows: CHBr_3 from -79 to 187 nmol m^{-2}
48 d^{-1} (1.9 to 22.6 pptv), CH_2Br_2 from -55 to $71 \text{ nmol m}^{-2} \text{ d}^{-1}$ (0.7 to 19 pptv), CHBr_2Cl from -408
49 to $768 \text{ nmol m}^{-2} \text{ d}^{-1}$ (0.4 to 11 pptv), CHBrCl_2 from -29 to $45 \text{ nmol m}^{-2} \text{ d}^{-1}$ (0.5 to 9.6 pptv),
50 CHCl_3 from -577 to $883 \text{ nmol m}^{-2} \text{ d}^{-1}$ (15 to 57 pptv), C_2HCl_3 from -74 to $884 \text{ nmol m}^{-2} \text{ d}^{-1}$ (0.4
51 to 11 pptv), methyl chloride (CH_3Cl) from -5300 to $10,800 \text{ nmol m}^{-2} \text{ d}^{-1}$ (530 to 730 pptv),
52 methyl bromide (CH_3Br) from -111 to $118 \text{ nmol m}^{-2} \text{ d}^{-1}$ (7.5 to 14 pptv) and methyl iodide
53 (CH_3I) from -25 to $17 \text{ nmol m}^{-2} \text{ d}^{-1}$ (0.4 to 2.8 pptv). Taking into account statistical
54 uncertainties, the coastal sites (particularly those where soil is mixed with salt deposits) were
55 identified as the source for all VHOCs, but this was not statistically significant for CHCl_3 .
56 Further away from the coastal area, the bare soil sites were sources for CHBrCl_2 , CHBr_2Cl ,
57 CHCl_3 , and probably also for CH_2Br_2 and CH_3I , and the agricultural sites were sources for
58 CHBr_3 , CHBr_2Cl and CHBrCl_2 . In contrast to previous reports, we also observed emissions of

59 brominated trihalomethanes, with net molar fluxes ordered as follows: $\text{CHBr}_2\text{Cl} > \text{CHCl}_3 >$
60 $\text{CHBr}_3 > \text{CHBrCl}_2$, and lowest positive flux incidence for CHCl_3 among all trihalomethanes; this
61 finding can be explained by the soil's enrichment with Br. Correlation analysis, in agreement
62 with recent studies, indicated common controls for the emission of CHBr_2Cl and CHBrCl_2 , and
63 likely also for CHBr_3 . There were no indications for correlation of the brominated
64 trihalomethanes with CHCl_3 . Also in line with previous reports, we observed elevated emissions
65 of CHCl_3 and C_2HCl_3 from mixtures of soil and different salt-deposited structures; the flux
66 correlations between these compounds and methyl halides (particularly CH_3I) suggested that at
67 least CH_3I is also emitted via similar mechanisms or is subjected to similar controls. Overall,
68 our results indicate elevated emission of VHOCs from bare soil under semiarid conditions.
69 Along with other recent studies, our findings point to the strong emission potential of a suite of
70 VHOCs from saline soils and salt lakes, and call for additional studies of emission rates and
71 mechanisms of VHOCs from saline soils and salt lakes.

72

73 **1 Introduction**

74 Volatile halogenated organic compounds (VHOCs), such as methyl halides (CH_3X ; X = Br, Cl
75 and I) and very short-lived halogenated substances (VSLs; lifetime <6 months) contribute
76 substantially to the loading of tropospheric and lower stratospheric reactive halogen species
77 containing Cl, Br or I and their oxides (Carpenter et al., 2014; Carpenter et al., 2013; Derendorp
78 et al., 2012). Reactive halogen species, in turn, lead to ozone (O_3) destruction, changes in
79 atmospheric oxidation capacity, and radiative forcing (Simpson et al., 2015). Depletion of O_3 in
80 the stratosphere is associated with damage to biological tissues owing to an increase in
81 transmittance of UVB radiation (Rousseaux et al., 1999). In the troposphere, O_3 destruction is of
82 great importance, given that O_3 is toxic to humans, plants and animals, is a greenhouse gas, and
83 plays a key role in the oxidation capacity of the atmosphere.

84 The lifetimes of VHOCs vary significantly (see summary in Table S1), which in turn affects
85 their influence in both the troposphere and the stratosphere. Owing to their relatively short
86 lifetimes (<6 months), the transport of VSLs to the stratosphere occurs primarily in the tropics,
87 where deep convection is frequent. Brominated VSLs originate primarily from the ocean,
88 whereas chlorinated VSLs, except for chloroform (CHCl₃) and chloroethane, originate
89 primarily from anthropogenic sources (Carpenter et al., 2014). Methyl iodide (CH₃I), having a
90 relatively short lifetime, is also classified as a VSL, and contributes significantly to
91 tropospheric O₃ destruction in the marine boundary layer (MBL) (Carpenter et al., 2014) and
92 also, indirectly, to the formation of cloud condensation nuclei (O'Dowd et al., 2002). It is now
93 well established that emission of brominated [e.g., bromoform (CHBr₃), methylene bromide
94 (CH₂Br₂), and dibromochloromethane (CHBr₂Cl)] and iodinated (e.g., CH₃I) VSLs tends to be
95 much greater in coastal areas than in the open ocean (Carpenter et al., 2009;Carpenter et al.,
96 2000;Liu et al., 2011;Bondu et al., 2008;Manley and Dastoor, 1988;Quack and Wallace, 2004),
97 since in the former they can also be emitted from macroalgae under oxidative stress at low tide
98 (Pedersen et al., 1996). The ocean is also a major source of methyl bromide (CH₃Br), and a
99 significant (~19%) source of methyl chloride (CH₃Cl) (Carpenter et al., 2014), as they originate
100 from phytoplankton, bacteria, and detritus.

101 Despite the numerous efforts made in recent years to evaluate halocarbon budgets,
102 uncertainties still exist concerning the strengths of both their sources and their sinks. The
103 budgets of CH₃Br and CH₃Cl are unbalanced, with sinks outweighing sources by ~32% and
104 ~17%, respectively (Carpenter et al., 2014). Uncertainties in the global budgets of naturally
105 occurring VSLs are large, with discrepancies having a factor of ~2–3 between top-down and
106 bottom-up emission inventories (Carpenter et al., 2014). This results largely from poor
107 characterization of emission sources (Warwick et al., 2006;Hossaini et al., 2013;Ziska et al.,
108 2013).

109 Studies over the past few decades have clearly demonstrated that terrestrial sources also
110 constitute a major fraction of the atmospheric budget for both methyl halides and VSLs
111 (Carpenter et al., 2014). Many terrestrial plants have been identified as sources of CH₃Cl
112 (Yokouchi et al., 2007), and the results of recent modeling indicate that about 55% of the global
113 sources of CH₃Cl originate from tropical lands (Xiao et al., 2010;Carpenter et al., 2014). It has
114 also been suggested that natural terrestrial sources of CH₃Br, especially emissions from
115 terrestrial vegetation, must account for a large part of the missing sources (Gebhardt et al.,
116 2008;Yassaa et al., 2009;Warwick et al., 2006;Gan et al., 1998;Yokouchi et al., 2002;Moore,
117 2006;Rhew et al., 2001;Wishkerman et al., 2008), and emissions have been observed from
118 peatlands, wetlands, salt marshes, shrublands, forests, and some cultivated crops (Gan et al.,
119 1998;Varner et al., 1999;Lee-Taylor and Holland, 2000). CHCl₃ has also been found to be
120 emitted from various terrestrial sources, including rice, soil, tundra, forest floor, and different
121 types of microorganisms, such as fungi and termites (see Dimmer et al. (2001) and (Rhew et al.,
122 2008)).

123 The importance of VHOC emission from soil, sediments, and salt lake deposits has been
124 recently recognized (see Kotte et al. (2012), Ruecker et al. (2014), and references therein). For
125 example, Keppler et al. (2000) revealed natural abiotic emission of CH₃Br, CH₃Cl, and CH₃I, as
126 well as additional chlorinated VHOCs from soil and sediments harboring an oxidant such as
127 Fe(III), halides, or organic matter (OM), while Weissflog et al. (2005) found that salt lake
128 sediments can be a source for several C1 and C2 chlorinated species, including CHCl₃ and
129 trichloroethylene (C₂HCl₃), induced by halobacteria in the presence of dissolved Fe. Huber et al.
130 (2009) identified abiotic natural emission of trihalomethanes from soil, including CHCl₃,
131 bromodichloromethane (CHBrCl₂), and CHBr₂Cl, induced by oxidation of OM by Fe(III) and
132 hydrogen peroxide, while Hoekstra et al. (1998) identified natural emission of CHBr₃ following
133 enrichment of the soil by potassium bromide. In addition, Carpenter et al. (2005) identified
134 CHBr₃ emission from peatland or another terrestrial source at Mace Head (inIreland). Albers et

135 al. (2017) revealed that CHCl_3 , CHBrCl_2 , and potentially also other trihalomethanes can be
136 emitted from soils, probably induced by hydrolysis of trihaloacetyl compounds. Several other
137 studies have reported strong emissions of CH_3Cl , CH_3Br , and CH_3I from coastal marsh
138 vegetation and to a lesser extent from the marsh soil (Rhew et al., 2002;Rhew et al., 2001;Rhew
139 et al., 2014;Wishkerman et al., 2008;Rhew et al., 2000), with significant importance on a global
140 scale (Deventer et al., 2018;Manley et al., 2006). In addition, peatland has been indicated as an
141 important source for CH_3Br , CH_3Cl , CH_3I and CHCl_3 (Simmonds et al., 2010;Khan et al.,
142 2012;Dimmer et al., 2001;Carpenter et al., 2005), and Sive et al. (2007) identified a globally
143 significant source of CH_3I from mid-latitude vegetation and soil.

144 Accordingly, the need for improved understanding of VHOC emissions from saline
145 environments and their potential importance on the global scale have been highlighted by recent
146 studies (Weissflog et al., 2005;Kotte et al., 2012;Ruecker et al., 2014;Deventer et al., 2018).
147 Moreover, due to global warming, saline environments are likely to become more prevalent (IPCC
148 2007;Ruecker et al., 2014). The present study is aimed at improving our knowledge of the
149 emission of VHOCs from salt lake environments by quantifying the flux and mixing ratios of
150 methyl halides and halogenated VSLs from different sites in the area of the Dead Sea.

151 The Dead Sea is unique because it is the lowest point on the Earth's surface, about 430 m
152 below sea level, with water salinity 12 times higher and a bromide (Br^-) to chloride (Cl^-) ratio
153 (Br^-/Cl^-) 7.5 times higher than in normal ocean waters. Fast evaporation from the sea leads to a
154 variety of newly exposed sea deposits. Despite the high salinity, emission of VHOCs via biotic
155 processes at the Dead Sea is also potentially feasible. The unicellular green alga *Dunaliella*
156 *parva* has been found to be active in Dead Sea water (Oren and Shilo, 1985), while additional
157 bacteria and fungi that have been isolated from the sea could also potentially be active under the
158 Dead Sea's extreme conditions (Oren et al., 2008;Jacob et al., 2017;Buchalo et al., 1998).
159 Mycobiota, including fungi and biota, have also been detected in the Dead Sea's hypersaline soil
160 and coastal sand (Pen-Mouratov et al., 2010;Kis-Papo et al., 2001;Jacob et al., 2017).

161 Studying the emission of VHOCs at the Dead Sea is also fundamental for understanding
162 local surface O₃-depletion events (Hebestreit et al., 1999;Tas et al., 2003;Matveev et al.,
163 2001;Zingler and Platt, 2005;Tas et al., 2006) as well as mercury-depletion events (Tas et al.,
164 2012;Obrist et al., 2011) in the boundary layer of this area. Emissions of brominated and
165 iodinated VHOCs can potentially lead to formation of the reactive iodine and bromine species
166 that are responsible for these processes.

167

168 **2 Methods**

169 **2.1 Field measurements and sampling**

170 Field measurements were taken at selected sites along the Dead Sea to measure the mixing
171 ratios and evaluate the vertical flux of VHOCs over different land-use types, seasons, and
172 distance from the seawater, as summarized in Table 1. Soil samples from the various sites were
173 analyzed and meteorological measurements were performed in situ.

174

175 **2.1.1 Measurement sites**

176 All measurements were taken in the Dead Sea area. The Dead Sea's geographical position is
177 between 31°00' N and 31°50' N at 35°30' E, about 430 m below sea level. It is located in a
178 semiarid area, with mean daily maximum temperatures for summer and winter of ~40 °C and
179 ~21 °C, respectively. The Dead Sea has low rates of freshwater inflow and precipitation (20–50
180 mm y⁻¹; Shafir and Alpert, 2010), while seawater evaporation rates are high, estimated at about
181 400 cm y⁻¹ (Alpert et al., 1997). As a result, the water salinity is 12 times higher than the average
182 salinity of ocean water. Dead Sea water contains on average 5.6 g L⁻¹ Br⁻ and 225 g L⁻¹ Cl⁻ (Br⁻
183 /Cl⁻ ≈ 0.025) (Niemi, 1997), whereas normal ocean water contains 0.065 g L⁻¹ Br⁻ and 19 g L⁻¹
184 Cl⁻ (Br⁻/Cl⁻ ≈ 0.0034) (Sverdrup, 1942). The main anthropogenic emission source in the area,
185 apart from local transportation and a few small settlements, is the Dead Sea Works, a potash
186 plant located to the south of most of the measurement sites (see Fig. 1). Agricultural fields,

187 which are mostly concentrated in the north near Kalya, in the south near Ein Tamar and near Ein
188 Gedi (see Fig. 1), are also potential sources for the emission of VHOCs in the area. To the best
189 of our knowledge, there are no wastewater facilities near the Dead Sea area, which could
190 otherwise also contribute to the emission of VHOCs such as CHCl_3 and CHBr_3 .

191 All measurement sites were nearly flat, homogeneous and located either along or near the
192 Dead Sea coast (see Fig. 1). Sites were classified according to surface cover: bare soil sites at
193 Mishmar (BARE-MSMR) and at Masada (BARE-MSD); coastal sites that are mixtures of soil
194 and salt deposits at Ein Gedi (COAST-EGD) and Tzukim (COAST-TKM); natural *Tamarix*
195 vegetation at Ein Tamar (TMRX-ET); irrigated agricultural watermelon field at Kalya
196 (WM-KLY); and seawater at Kedem (SEA-KDM). Note that at SEA-KDM, we did not
197 evaluate fluxes. Based on in situ wind-direction measurements, the sampled air masses at
198 SEA-KDM were transported over the seawater from the east (see Fig. 1) at least 1 h prior to
199 sampling and during the sampling. To study the effect of distance from the seawater on emission
200 rates, measurements at both COAST-EGD and COAST-TKM were taken at three and two
201 different distances from the sea, respectively. The shorter, middle, and longer distances from the
202 seawater were termed, respectively, SD, MD and LD. Emission rates at both COAST-EGD and
203 COAST-TKM could potentially be affected by distance from the seashore; there are several
204 reasons for this, including changes across the sites in soil salt and water content and changes in
205 density of the extremely sparse vegetation cover. In addition, depending on the local wind
206 direction at COAST-TKM-SD and COAST-EGD-SD, direct emission and uptake from the
207 seawater can potentially affect the samples.

208 In the following, we briefly describe the different measurement sites; additional information
209 about the sites and measurements is provided in Table 1. BARE-MSMR has a bare soil
210 consisting of loess and a small fraction of drifted soil covered with small stones and extremely
211 sparse vegetation, and is located in a valley 1.5 km to the west of the Dead Sea shore. BARE-
212 MSD has bare Hamada soil, with small stones and loess, and is located 2.1 km to the west of the

213 Dead Sea. COAST-EGD-SD has a dried-out bare saline soil, mixed with salty beds and rocks
214 with a small contribution of freshwater inflow. COAST-EGD-MD has a dried-out sea bed of
215 bare saline soil, mixed with salty beds and rocks, 0.3 km west of the Dead Sea shore.
216 COAST-EGD-LD is a dried-out sea bed of loess saline bare soil, mixed with drifted soil, 0.8
217 km from the Dead Sea shore. COAST-TKM-SD is a wetted bare soil with salt deposits,
218 groundwater inflow from the Dead Sea, and minor (<5%) freshwater inflow lines covered with
219 perennial grasses found in wetlands (e.g., *Phragmites* sp.), about 0.5 km from the shore.
220 COAST-TKM-LD is a flat rocky loess area about 1.5 km from the shore, with patchy salts and
221 sparse mixed shallow vegetation, mostly small *Atriplex* sp., *Tamarix* sp. and *Retama raetam*.
222 TMRX-ET is a moderately dense *Tamarix* grove, of 4–5 m average height, ~2.25 km² and 60–
223 70% vegetation cover fraction, with sandy soil, located 1.7 km south of the southern tip of the
224 Dead Sea evaporation ponds (see Fig. 1). Lastly, WM-KLY is a well-irrigated and flat 700 x
225 350 m² agricultural field with cultivated watermelon surrounded by a larger agricultural area of
226 ~3 km², located 2.5 km northwest of the Dead Sea shore (Fig. 1). The watermelon crop had an
227 average height of ~0.67 m and 95–99% vegetation cover.

228

229 **2.1.2 Field measurements and sampled air analysis**

230 Air was sampled at each site by placing three different canisters at specified heights (see Table
231 1) along a meteorological tower. The samples were used to quantify the mixing ratios of
232 different VHOCs in the air, and their corresponding fluxes were calculated by applying the flux-
233 gradient method (see (Stull 1988;Maier and Schack-Kirchner, 2014;Meredith et al., 2014)). By
234 default, the differences in height between the canisters increased exponentially with height,
235 considering the typical decrease in the vertical gradient of emitted species in the surface layer
236 (Stull 1988). All canisters were placed high enough above the ground to ensure that all sampling
237 was performed within the inertial sublayer, except for the lowest canister at TMRX-ET. In all
238 cases, the sample footprint fell inside the target fetch, except for the sampling at COAST-EGD,

239 for which the sample footprint included a narrow strip of the seawater (estimated at about 40%
240 of the footprint). To minimize non-synchronized air sampling by the three canisters, we
241 constructed a special sampling system that allows almost simultaneous filling of the canisters.
242 For each sample, air was drawn into a 1.9 L stainless-steel canister via passive grab samplers
243 (Restek Corporation, PA, USA), resulting in a sampling duration of 20 min and internal canister
244 pressures higher than 600 Torr. Meteorological parameters, including temperature and relative
245 humidity, wind speed and direction, and global solar radiation, were all continuously measured,
246 starting at least 30 min before air sampling was initiated (summarized in Table S6). All canisters
247 were sent to the Blake/Rowland group, University of California, Irvine, where they were
248 analyzed by techniques similar to those described in Colman et al. (2001). Analyses were
249 performed using gas chromatography combined with mass spectrometry, flame-ionization
250 detection and electron-capture detection to quantify the air mixing ratios of CHBr_3 , C_2HCl_3 ,
251 CH_2Br_2 , CHBr_2Cl , CHBrCl_2 , CHCl_3 , CH_3I , CH_3Br and CH_3Cl . For all gases, accuracy ranged
252 between 1% and 10% and analytical precision between 1% and 5% (see Table S2). Note that the
253 lower-height canister analysis for COAST-TKM-LD-s and the mid-height canister analysis of
254 TMRX-ET-1 indicated an outlier mixing ratio for all VHOCs and for CH_3Cl , respectively ($p \ll$
255 0.01; Grubbs test; (Grubbs and Beck, 1972)). We therefore excluded the lower-height
256 COAST-TKM-LD-s measurement from all of our calculations and used only the lowest and
257 highest canisters in the flux calculation for TMRX-ET-1, as indicated in all relevant figures and
258 tables.

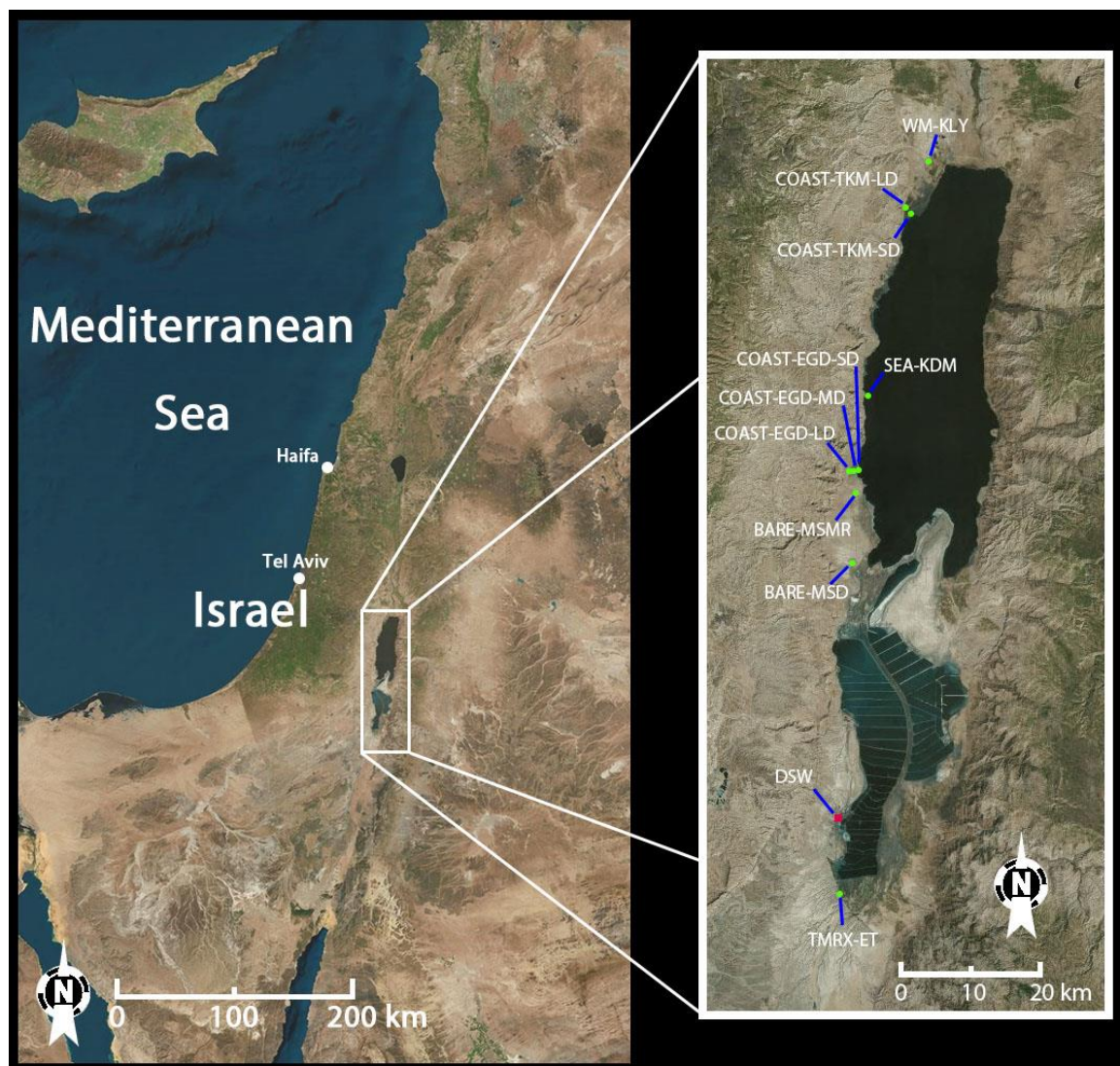
259 **Table 1.** Summary of VHOC samplings at the Dead Sea. Shown are the date, time and site name (and abbreviation)
 260 for the sample, sampling height, total number of samplings for each experiment and whether the sample could
 261 potentially have been influenced by emission from the seawater and by precipitation prior to sampling.

Date dd/m/yyyy	Time (local)	Site name / measurement abbreviation ^a	Sampling height (m)	Total samplings	Seawater ^b	Precipitation (days before sampling) ^c
20/4/2016	08:45–08:55	BARE–MSMR / BARE–MSMR-1	2.5, 4.5, 7.0	3	–	>3 months
21/4/2016	08:45–08:55	WM–KLY / WM–KLY-1	1.0, 2.0, 4.0	3	–	>3 months
02/5/2016	08:45–08:55	TMRX–ET / TMRX–ET-1	4.5, 5.5, 7.5	3*	–	>3 months
03/5/2016	08:45–08:55	WM–KLY / WM–KLY-2	1.0, 2.0, 4.0	3	–	>3 months
25/5/2016	08:30–08:40	BARE–MSD / BARE–MSD-1	1.25, 2.5, 5	3	–	1–2
26/5/2016	08:30–08:40	BARE–MSD / BARE–MSD-2	1.25, 2.5, 5	3	–	2–3
30/5/2016	12:00–12:10	TMRX–ET / TMRX–ET-2	4.5, 5.5, 7.5	3	–	>3 months
31/5/2016	12:00–12:10	BARE–MSMR / BARE–MSMR-2	2.5, 4.5, 7	3	–	>3 months
11/7/2016	12:00–12:20	BARE–MSD / BARE–MSD-3	1.25, 2.5, 5	3	–	>3 months
11/7/2016	18:00–18:20	BARE–MSD / BARE–MSD-4	1.25, 2.5, 5	3	–	>3 months
21/2/2017	11:20–11:40	COAST–TKM–SD / COAST–TKM–SD–w	1, 2.5, 6.5	3	+/-	5
22/2/2017	11:00–11:20	COAST–TKM–LD / COAST–TKM–LD–w	1.5, 3, 7	3	–	6
28/2/2017	11:20–11:40	COAST–EGD–SD / COAST–EGD–SD–w	1, 2.5, 6.5	3	+	0
01/3/2017	11:07–11:27	COAST–EGD–MD / COAST–EGD–MD–w	1, 2.5, 6.5	3	+/-	>3 months
02/3/2017	11:00–11:20	COAST–EGD–LD / COAST–EGD–LD–w	1, 2.5, 6.5	3	–	>3 months
02/3/2017	12:55–13:15	SEA–KDM / SEA–KDM–w	1	1	+	>3 months
25/4/2017	11:30–11:50	COAS–EGD–SD / COAST–EGD–SD–s	1, 2.5, 6.5	3	+	>3 months
26/4/2017	11:00–11:20	COAST–EGD–MD / COAST–EGD–MD–s	1, 2.5, 6.5	3	+/-	>3 months
27/4/2017	11:00–11:20	COAST–EGD–LD / COAST–EGD–LD–s	1, 2.5, 6.5	3	–	>3 months
03/5/2017	12:10–12:30	COAST–TKM–SD / COAST–TKM–SD–s	1, 2.5, 6.5	3	–	>3 months
04/5/2017	10:30–10:50	COAST–TKM–LD / COAST–TKM–LD–s	1.5, 3, 7	3**	–	>3 months
04/5/2017	12:30–12:50	SEA–KDM / SEA–KDM–s	1	1	+	>3 months

262 ^a The suffixes "s" and "w" refer to samples taken during the spring and winter, respectively. SD, MD, and LD refer
 263 to relatively short, medium, and long distance from the coastline, respectively (see Sect. 2.1).

264 ^b "+", "–" and "+/–" indicate that the samplings were, could not be, or may be influenced by emission from the
 265 seawater, respectively.

266 ° Values indicate the number of days before sampling on which precipitation occurred.
 267 Additional abbreviations: MSD, Masada; MSMR, Mishmar; KLY, Kalya; ET, Ein Tamar; KDM, Kedem; EGD,
 268 Ein Gedi; BARE, bare soil site; COAST, coastal soil–salt mixture site; WM, agricultural cultivated watermelon
 269 site; TMRX, natural *Tamarix* site; SEA, sampling near the seawater (see Sect. 2.1.1).
 270 *Samples exclude one CH₃Cl measurement in TMRX–ET-1 (see Sect. 2.1.2).
 271 ** Samples exclude one measurement for all VHOCs (see Sect. 2.1.2).
 272



273
 274 **Figure 1.** Location and satellite image of the Dead Sea measurement sites (see Sect. 2.1.2) and Dead Sea Works
 275 (DSW). Left: location of the Dead Sea. Right: zoom-in on the area of the measurement sites.

276
 277 **2.2 Vertical flux evaluation**

278 The vertical flux, F_c , of a species c , was evaluated according to the gradient approach using the
 279 vertical gradient of c , $\frac{\partial c}{\partial z}$, and a constant, K_c :

$$F_c \equiv -K_c \frac{\partial C}{\partial z} \quad (1)$$

280 K_c represents the rate of turbulent exchange in Eq. 1 and was evaluated on the basis of the
 281 Monin–Obukhov similarity theory (MOST) described by Lenschow (1995):

$$K_{C(z)} = u_* K Z \phi_c(\zeta) \quad (2)$$

283 where u_* is the friction velocity, K is the Von Kármán constant, Z is the measurement height
 284 and ϕ_c is a universal function of the dimensionless parameter ζ . According to MOST, vertical
 285 fluxes in the surface layer can be evaluated on the basis of the dimensionless length parameter,
 286 ζ , according to

$$\zeta = (z - d)/L \quad (3)$$

288 where z , d and L are the vertical coordinate, zero displacement, and the Monin–Obukhov length,
 289 respectively (Schmugge and André, 1991).

290 We relied on the commonly used assumption that ϕ_c is similar to ϕ_h for chemical species
 291 with a relatively long lifetime (Dearellano et al., 1995), and calculated ϕ_h using the following
 292 equation for the relationship between ϕ_h and ζ , which was found to be valid for $0.004 \leq -z/L \leq$
 293 4 (Dyer and Bradley, 1982; Yang et al., 2001):

$$\phi_h = (1 - 14\zeta)^{-1/2} \quad (4)$$

295 We derived L from the Pasquill and Gifford stability class (Pasquill and Smith, 1971) and
 296 roughness length (z_0) according to Golder (1972). z_0 was evaluated based on the specific surface
 297 characteristics at each site using information provided by the WMO (2008). The stability class
 298 was evaluated using the in situ-measured solar radiation and wind speed (Gifford, 2000; Pasquill
 299 and Smith, 1971). u_* was derived from the logarithmic wind profile according to MOST, using
 300 the following equation:

301
$$u(z) = \frac{u^*}{k} \ln\left(\frac{z-d}{z_0}\right) \quad (5)$$

302 where $u(z)$ is the wind speed at height z , and ψ_m is a correction for diabatic effect on momentum
 303 transport. Using the measured u at a height of 10 m, we calculated the wind speed at each
 304 measurement height according to Gualtieri and Secci (2011):

305
$$u_2 = u_1 \frac{\ln(z_2/z_0) - \psi_m(z_2/L)}{\ln(z_1/z_0) - \psi_m(z_1/L)} \quad (6)$$

306 where ψ_m is calculated using:

307
$$\Psi_m(Z/L) = 2\ln(1 + X/2) + \ln(1 + X^2/2) - 2\arctan(X) + \pi/2 \quad (7)$$

308 and
$$X = \left(1 - 15\left(\frac{Z}{L}\right)\right)^{1/4} \quad (8)$$

309

310 2.3 Soil analyses

311 Soil samples at each site were collected up to a depth of 5 cm during the summer, at least 3
 312 months after any rain event in the Dead Sea area, to ensure no impact on the samples by recent
 313 drift and percolation. The samples were analyzed for Br, Cl, I, OM, moisture and Fe in the soil,
 314 as well as for soil pH. Prior to halide quantification, extractions for each sample were prepared
 315 using HNO₃ (BCE, 1990). Total Br and I were quantified using inductively coupled plasma
 316 mass spectrometry (ICP–MS). Total Cl was quantified by potentiometric titration against
 317 AgNO₃.

318 To quantify Fe in the soil, microwave-assisted digestion with reverse aqua regia was used,
 319 and Fe concentration was determined by inductively coupled plasma optical emission
 320 spectrometry (ICP–OES). A batch of each sample (~300 mg of dry soil) was digested in reverse
 321 aqua regia (HNO₃ (65%):HCl (30%); 3:1 mixture, v/v). Digestion was allowed to proceed in
 322 quartz vessels using a Discover sample digestion system at high temperature and pressure (CEM
 323 Corporation, NC, USA). The vessels were cooled and the volume was brought to 20 mL with
 324 deionized water. Element concentrations were measured in clear solutions using high-resolution

325 dual-view ICP–OES PlasmaQuant PQ 9000 Elite (Analytik Jena, Germany). The reported
326 values represent the lower limit, because the samples were not completely dissolved. Soil water
327 content and OM were determined by weight loss under dry combustion at 105 °C and 400 °C,
328 respectively. Soil pH was measured in 1:1 (v/v) soil-to-water extracts with a model 420 pH
329 meter (Thermo Orion, MA, USA).

330

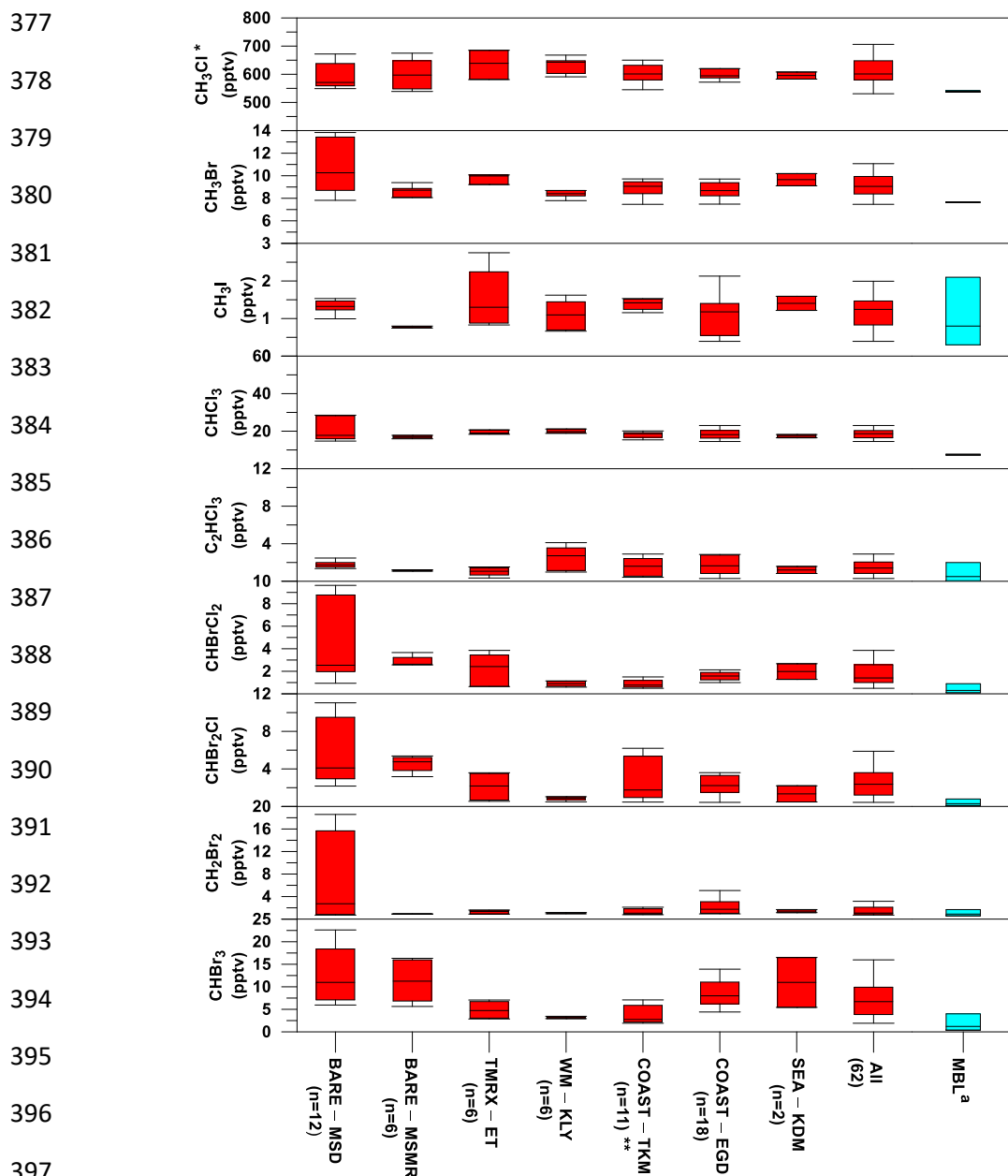
331 **3 Results and discussion**

332 **3.1 VHOC flux and mixing ratio**

333 Overall, the measurements at the Dead Sea boundary layer revealed higher mixing ratios for all
334 investigated VHOCs than their expected levels at the Mediterranean Sea and Red Sea MBL,
335 indicating higher local emissions from the Dead Sea area. No association was observed between
336 the measured mixing ratios and the air masses flowing from the direction of the Dead Sea
337 Works (see Sect. S5 for anthropogenic impact), a potash plant located to the northwest of the
338 TMRX–ET site and to the south of all other measurement sites (see Fig. 1) that is the main
339 anthropogenic source in the area under investigation. Furthermore, the correlation analysis
340 (Table S5) revealed that only C_2HCl_3 was associated with C_2Cl_4 , a well-known anthropogenic
341 VHOC. The absence of any other associations suggested dominance of natural sources for the
342 VHOCs in the studied area. The measured mixing ratios for the different species at the
343 measurement sites are summarized and compared with mixing ratios from the MBL in Table S3
344 and in Fig. 2. The figure indicates that median mixing ratios measured at the Dead Sea were
345 generally higher than the corresponding mixing ratios in the MBL. Our calculations suggest that
346 the mixing ratios at the Dead Sea are higher by factors of 1.2–8.0 for brominated and
347 chlorinated VSLs and ~1.5, 1.3 and 1.1 for CH_3I , CH_3Br and CH_3Cl , respectively. It should be
348 noted, however, that while Fig. 2 implies elevated VHOC emission from the Dead Sea,
349 comparison of mean or median mixing ratios of VHOCs for the Dead Sea with those for the
350 MBL is not straightforward, considering that VHOC mixing ratios in the MBL are sensitive to

351 several factors, including season and latitude. Moreover, the measurement height can play a
352 significant role in affecting the mixing ratios due to decreasing mixing ratios with height over
353 areas where local emissions occur. Hence, we also compared the measured fluxes and mixing
354 ratios with their corresponding values measured in coastal areas, where the highest mixing ratios
355 in the MBL were generally measured due to stronger emissions. The measured mixing ratios
356 and fluxes at the Dead Sea were in most cases comparable to or higher than in coastal areas.

357 Owing to their large contribution to stratospheric Br, CHBr_3 and CH_2Br_2 are the most
358 extensively studied VSLs in the MBL (Hossaini et al., 2010). The mixing ratios of CHBr_3 and
359 CH_2Br_2 that we measured at the Dead Sea ranged from 1.9 to 22.6 pptv and from 0.7 to 18.6
360 pptv, respectively, higher than most of their reported mixing ratios in coastal areas where the
361 highest mixing ratios have typically been measured. For example, Carpenter et al. (2009)
362 reported elevated mixing ratios for CHBr_3 and CH_2Br_2 along the eastern Atlantic coast ranging
363 from 1.9 to 4.9 and from 0.9 to 1.4 ppt, respectively, and Nadzir et al. (2014) reported mixing
364 ratios of 0.82–5.25 pptv and 0.90–1.92 ppt for CHBr_3 and CH_2Br_2 , respectively, for several
365 tropical coastal areas, including the Strait of Malacca, the South China Sea and the Sulu–
366 Sulawesi Sea. Somewhat higher mixing ratios for CHBr_3 have been measured in only a few
367 locations, including some in coastal areas near New Hampshire (Zhou et al., 2008), San
368 Cristobal Island (Yokouchi et al., 2005; O'Brien et al., 2009), Cape Verde (O'Brien et al., 2009),
369 Borneo (Pyle et al., 2011), Cape Point (Kuyper et al., 2018; Butler et al., 2007), and at the
370 Atmospheric Observing Station at Thompson Farm in New Hampshire, USA (TF) during the
371 summer (Zhou et al., 2005), whereas the range (and average) concentrations at those locations
372 were 0.2–37.9 pptv (5.6–6.3), 4.2–43.6 pptv (14.2), 2.0–43.7 pptv (4.3–13.5), 0.2–60 pptv
373 (1.3–1.7), 4.4–64.6 pptv (24.8) and 0.6–37.9 pptv (2.6–5.9), respectively. For CH_2Br_2 , the
374 corresponding mixing ratios were reported as 1.3–2.3 pptv, 0.5–4.1 pptv, 0.7–8.8 pptv and 0.4–
375 4.2 pptv in New Hampshire, San Cristobal Island, Cape Verde and TF, respectively, which are
376 comparable with the mixing ratios measured at the Dead Sea.



398 **Figure 2.** Comparison of VHOC mixing ratios (in pptv) measured at the Dead Sea with their corresponding values
 399 at the marine boundary layer (MBL). For the Dead Sea sites, boxes indicate median, upper, and lower quartiles, and
 400 bars show minimum and maximum VHOC mixing ratios (see Table 1 for site abbreviations; "n" specifies the
 401 number of samples for each site). For the MBL, boxes indicate the median, minimum and maximum mixing ratios
 402 reported by Carpenter et al. (2014). ^a Values for CH₃Cl and CH₃Br represent mean and range for 2012 based on
 403 flask measurements by the US National Oceanic and Atmospheric Administration (NOAA)
 404 (<http://www.esrl.noaa.gov/gmd/dv/site/>) and in situ measurements by the Advanced Global Atmospheric Gases
 405 Experiment (AGAGE) (<http://agage.eas.gatech.edu/>), which were performed at ground stations, not in all cases
 406 representing the MBL. *Related CH₃Cl measurement excludes one sample at TMRX-ET-1 (see Sect. 2.1.2).
 407 **Related measurements exclude one sample for all VHOCs (see Sect. 2.1.2).

408 Table 2 presents the measured fluxes of all VHOCs studied, alongside the corresponding
409 statistical significance for a specific species' emission or depletion to a specific site. Note that
410 considering the similar characteristics of the two SD sites, and of the two BARE sites, we
411 assumed a common emission source from the two sites, in both cases, in evaluating the
412 statistical significance for these sites being a net source or net sink for the studied species.
413 Considering the small number of measurements at each site, the table classifies the statistical
414 significance of the fluxes' negative or positive values at a specific site into four different
415 categories. While p -values <0.05 are used here to indicate statistical significance, p -values of
416 <0.1 and <0.15 are also indicated when present.

417 Figure 3 presents the measured fluxes of all VHOCs studied, individually for statistically
418 significant and non-significant fluxes emitted or depleted to a specific site. Non-significant
419 fluxes are marked with black and gray for $0.05 < p < 0.1$ and $p > 0.1$, respectively. It can be seen
420 that for all species, at least one of the six studied areas could be classified as a net source, with
421 somewhat less sites being statistically significant net sources for CHCl_3 , C_2HCl_3 and CH_3I . Note
422 that as explained above, C_2HCl_3 was found to be affected by anthropogenic emission, which
423 could explain the relatively less frequent identified emissions for this species. Figure 3 clearly
424 demonstrates that the COAST sites, and particularly the SD sites, are associated with the highest
425 number of VHOCs with positive flux. These sites were also found as a source for CHCl_3 ,
426 C_2HCl_3 and CH_3I . Figure 3 does not indicate elevated VHOC emissions from the vegetated sites
427 (WM–KLY and TMRX–ET) compared to the BARE sites.

428 The flux magnitudes for CHBr_3 and CH_2Br_2 were greater than for most reported emissions
429 in the MBL (e.g., CHBr_3 , 25.2–62.88 $\text{nmol m}^{-2} \text{d}^{-1}$ for the Mauritanian upwelling (Quack et al.,
430 2007); CH_2Br_2 , 0.14–0.29 $\text{nmol m}^{-2} \text{d}^{-1}$ for the New Hampshire coast (Zhou et al., 2008)), but
431 were smaller than the corresponding average fluxes estimated by Butler et al. (2007) for global
432 coastal areas (~ 220 and $110 \text{ nmol m}^{-2} \text{d}^{-1}$, respectively) and than the average flux from the New

433 Hampshire coast as reported by Zhou et al. (2005) ($\sim 620 \pm 1370 \text{ nmol m}^{-2} \text{ d}^{-1}$ and 113 ± 130
434 $\text{nmol m}^{-2} \text{ d}^{-1}$, respectively).

435 Relatively high positive CHCl_3 fluxes were measured for BARE-MSMR ($247 \text{ nmol m}^{-2} \text{ d}^{-1}$),
436 TMRX-ET-2 ($213 \text{ nmol m}^{-2} \text{ d}^{-1}$) and COAST-EGD-SD-s ($883 \text{ nmol m}^{-2} \text{ d}^{-1}$), although the latter
437 two sites were not identified as a net source for CHCl_3 (Table 2). For comparison, the emission
438 from BARE-MSMR-1 was similar to the maximum emission found for tundra peat by Rhew et
439 al. (2008), whereas the average emissions from COAST-EGD-SD-s and TMRX-ET-2 were
440 higher than those from temperate peatlands ($\sim 496 \text{ nmol m}^{-2} \text{ d}^{-1}$ as measured by Dimmer et al.
441 (2001)). Whereas emissions for COAST-EGD-SD-s and TMRX-ET-2 might have been
442 affected by seawater and vegetation, respectively, the emission for BARE-MSMR can be
443 completely attributed to soil. The latter emission flux in BARE-MSMR was higher than the
444 maximum emission rate in arctic and subarctic soils ($\sim 115 \text{ nmol m}^{-2} \text{ d}^{-1}$) reported by Albers et
445 al. (2017).

446 All investigated site types, except for the natural vegetation (TMRX-ET), were identified as
447 net sources for CHBr_2Cl and CHBrCl_2 (Fig. 3). The mixing ratios of CHBr_2Cl and CHBrCl_2
448 were higher by factors of ~ 4 – 14 and ~ 5 – 11 , respectively, than the average reported values for
449 the MBL, and were also higher than the mixing ratios measured in nearby coastal areas, except
450 for the extremely high CHBr_2Cl mixing ratios attributed to emission from a rock pool at Gran
451 Canaria (ranging from 19 to 130 ppt; (Ekdahl et al., 1998)). For example, Brinckmann et al.
452 (2012) found mean mixing ratios for CHBr_2Cl and CHBrCl_2 in coastal areas of the Sylt Islands
453 (North Sea) of up to 0.2 and 0.1 ppt, respectively, while Nadzir et al. (2014) found CHBr_2Cl and
454 CHBrCl_2 mixing ratios of 0.07–0.15 ppt and 0.15–0.22 ppt, respectively, in the tropics. The
455 measured CHBr_2Cl fluxes for the Dead Sea were also higher than the reported value of 0.8
456 (range -1.2–10.8) $\text{nmol m}^{-2} \text{ d}^{-1}$ at coastal areas sampled during the Gulf of Mexico and East
457 Coast Carbon cruise (GOMECC), (Liu et al., 2011). Typically, the net CHBrCl_2 flux at the Dead

458 Sea was significantly higher than corresponding fluxes from arctic and subarctic soils, as
459 recently reported by Albers et al. (2017), ranging from 0.03–5.27 nmol m⁻² d⁻¹.

460 COAST–TKM and COAST–EGD-SD were found to be the only net source sites for CH₃Cl.
461 The highest positive fluxes were measured at COAST–EGD-SD and COAST–TKM-SD, with
462 maximum net fluxes of ~10,800 and 4900 nmol m⁻² d⁻¹, respectively. These fluxes are
463 comparable in magnitude to those reported for several terrestrial sources, such as tropical forests
464 (~4520 nmol m⁻² d⁻¹) by Gebhardt et al. (2008) or by Yokouchi et al. (2002), and for other
465 tropical or subtropical vegetation (Yokouchi et al., 2007), and they are higher than emissions
466 from dryland ecosystems, including shortgrass steppe or shrublands (Rhew et al., 2001). In some
467 cases, the measured fluxes were higher than average emissions from salt marshes (e.g., ~7300
468 nmol m⁻² d⁻¹; (Deventer et al., 2018)), but significantly smaller than the maximum fluxes from
469 salt marshes (e.g., 570,000 nmol m⁻² d⁻¹; (Rhew et al., 2000)).

470 Both COAST–TKM and COAST–EGD sites were identified as net sources, and with less
471 statistical significance ($p \leq 0.1$) also BARE–MSMR, for CH₃Br (Table 2). In contrast to CH₃Cl,
472 emissions of CH₃Br at the Dead Sea were significantly lower than the average reported
473 emissions from marshes (e.g., ~600 nmol m⁻² d⁻¹; (Deventer et al., 2018)). The fluxes measured
474 at the Dead Sea were also lower than the reported emission from a coastal beach in a Japanese
475 archipelago island (~53,000 nmol m⁻² d⁻¹), but higher, in most cases, than in other dryland
476 ecosystems (see Rhew et al. (2001)).

477 Similar to CH₃Br and CH₃Cl, for CH₃I, COAST–TKM and COAST–EGD, and particularly
478 the SD sites, were identified as net sources (Table 2). BARE–MSMR was also identified as a
479 net source for CH₃I. Positive measured net fluxes of this compound were in most cases
480 comparable to other reported fluxes over soil and vegetation. For example, Sive et al. (2007)
481 reported a CH₃I flux of ~18.7 nmol m⁻² d⁻¹ over soil and vegetation at TF, and a somewhat lower
482 emission (~12.6 nmol m⁻² d⁻¹) in Duke Forest, NC, USA. While the elevated flux at
483 COAST–EGD-SD-s (17.0 nmol m⁻² d⁻¹) could potentially have been affected by flow of the

484 sampled air over the seawater, the positive net fluxes at BARE–MSMR (1.00 and 4.42 nmol m⁻²
485 d⁻¹) indicate significant emission from bare soil at the Dead Sea. The positive fluxes measured at
486 BARE–MSMR were similar to the measured soil-emission fluxes of CH₃I reported by Sive et
487 al. (2007) at Duke Forest, averaging ~0.27 nmol m⁻² d⁻¹ (range, ~ 0.11–4.1 nmol m⁻² d⁻¹).

488 Only COAST–EGD and COAST-TKM-SD sites were found to be statistically
489 significant sources ($p < 0.05$, see Table 2) for C₂HCl₃, suggesting that the elevated mixing ratios
490 for this species in the Dead Sea area result mostly from local anthropogenic emissions. This
491 possibility is supported by the high correlations with C₂Cl₄ (Table S5). Emissions from a more
492 distant natural source, such as the Mediterranean Sea or Red Sea, are unlikely given their large
493 distance away (~90 km and ~160 km, respectively).

494 **Table 2.** VHOC fluxes for the different measurement sites. Shown are the measured flux ($\text{nmol m}^{-2} \text{d}^{-1}$) obtained
495 for the different measurements. Values in bold and in parentheses indicate that the related measurement site is a
496 significant ($p < 0.05$) or non-significant ($p > 0.15$) net source or sink for the specific VHOC based on one-sample t-
497 test. Additional categories are defined below. These calculations assume COAST-EGD-SD and COAST-TKM-SD
498 as the same source (see Section 2.1.2). Also shown are the average flux (mean) and average positive flux (mean
499 positive) for all species, as well as the percentage of incidence of positive flux (X) out of total measured fluxes,
500 individually for each site and each VHOC (See Table 1 for abbreviations of the different measurement sites). All
501 presented values, including mean, mean positive and X include only fluxes associated with $p < 0.05$ (bolded; S) and
502 values associated with $p \geq 0.05$ (presented in parentheses; NS), based on one-sample t-test.

Species Site	CH ₂ Br ₂	CHBr ₃	CHBr ₂ Cl	CHBrCl ₂	CHCl ₃	C ₂ HCl ₃	CH ₃ Cl	CH ₃ Br	CH ₃ I	X (%)	
BARE- MSMR-1	1.43	(-76.5)	-3.27	7.68	247	(7.33)	(2629)	71.9 ^a	4.42	33 (78)	
BARE- MSMR-2	1.51	(27.6)	21.3	19.9	6.51	(-10.4)	(-378)	12.6 ^a	1.00	44 (78)	
BARE- MSD-1	(-55.4)	(-37.7)	-3.58	1.32	(12.1)	-11.0 ^b	-1266	(5.26)	-0.73	11 (33)	
BARE- MSD-2	(23.5)	(103)	41.8	24.5	(-6.02)	-24.8 ^b	-1368	(-50.3)	-8.14	22 (44)	
BARE- MSD-3	(-0.60)	(32)	8.69	7.92	(-14.6)	4.32 ^b	311	(-47.9)	-2.95	22 (56)	
BARE- MSD-4	(-4.61)	(-1.41)	26.96	19.1	(64.7)	6.39 ^b	-472	(38.44)	-3.58	22 (56)	
COAST- EGD-SD-w	0.85	78.1	90.0	6.63	(-42.8)	47.3	-1040	88.4	1.45	78 (78)	
COAST- EGD-MD-w	-6.53	-79.0	187	23.1	(38.5)	37.5	(9719)	-111	-5.16 ^a	33 (56)	
COAST- EGD-LD-w	-16.7	88.7	768	-14.2	(-43.7)	-8.97	(-2281)	116	-24.5 ^a	33 (33)	
COAST- EGD-SD-s	3.71	187	72.3	14.8	883 ^b	884 ^a	10817	118	17.0	78 (100)	
COAST- EGD-MD-s	1.35	48.6	13.4	3.42	46.4 ^a	-8.39 ^b	(-530)	8.10	2.27	67 (78)	
COAST- EGD-LD-s	2.52	66.0	13.8	8.68	-40.8 ^a	-2.03 ^b	261 ^a	22.3	-2.96	56 (67)	
COAST- TKM-SD-w	-4.15 ^b	-28.1	123	1.62	22.8 ^a	0.89	4895	110	2.42	67 (78)	
COAST- TKM-LD-w	2.95	(28.5)	(-408)	(-6.2)	(-32.9)	-22.0 ^b	2200	57.3	(-1.03)	33 (44)	
COAST- TKM-SD-s	3.80 ^b	87.7	42.7	21.4	0.99 ^a	2.00	1210	49.3	-0.38	67 (89)	
COAST- TKM-LD-s*	0.56	(-3.83)	2.07 ^a	(1.67)	(12.6)	-0.31 ^b	1100	23.6	(0.97)	33 (78)	
TMRX- ET-1**	(-8.93)	(-23.0)	(-8.64)	(-28.5)	27.6 ^a	-0.36 ^b	(10500*)	(-90.8)	(-6.14)	0 (11)	
TMRX- ET-2	(70.6)	(73.7)	(20.4)	(45.4)	213 ^a	-4.53 ^b	(-5300)	(10.9)	(3.61)	0 (78)	
WM- KLY-1	1.45 ^a	50.7	2.09	8.57	(-577)	-74.1 ^b	(983)	(53.5)	-4.01	33 (56)	
WM- KLY-2	11.3 ^a	24.5	12.6	8.76	(6.31)	-20.0 ^b	(-4730)	(-31.6)	-8.29	33 (67)	
Mean	S NS	-0.84 (1.43)	52.4 (32.3)	88.5 (51.1)	10.2 (8.78)	70.9 (41.2)	-2.2 (40.1)	1640 (1360)	48.2 (22.7)	-2.75 (-1.74)	
Mean positive	S NS	1.86 (9.66)	78.9 (68.9)	102 (90.4)	11.8 (13.2)	127 (122)	21.9 (124)	3400 (4060)	65.9 (52.4)	6.17 (4.14)	
X (%)	S NS	40 (65)	40 (65)	70 (80)	75 (85)	10 (65)	20 (40)	30 (55)	45 (75)	20 (40)	

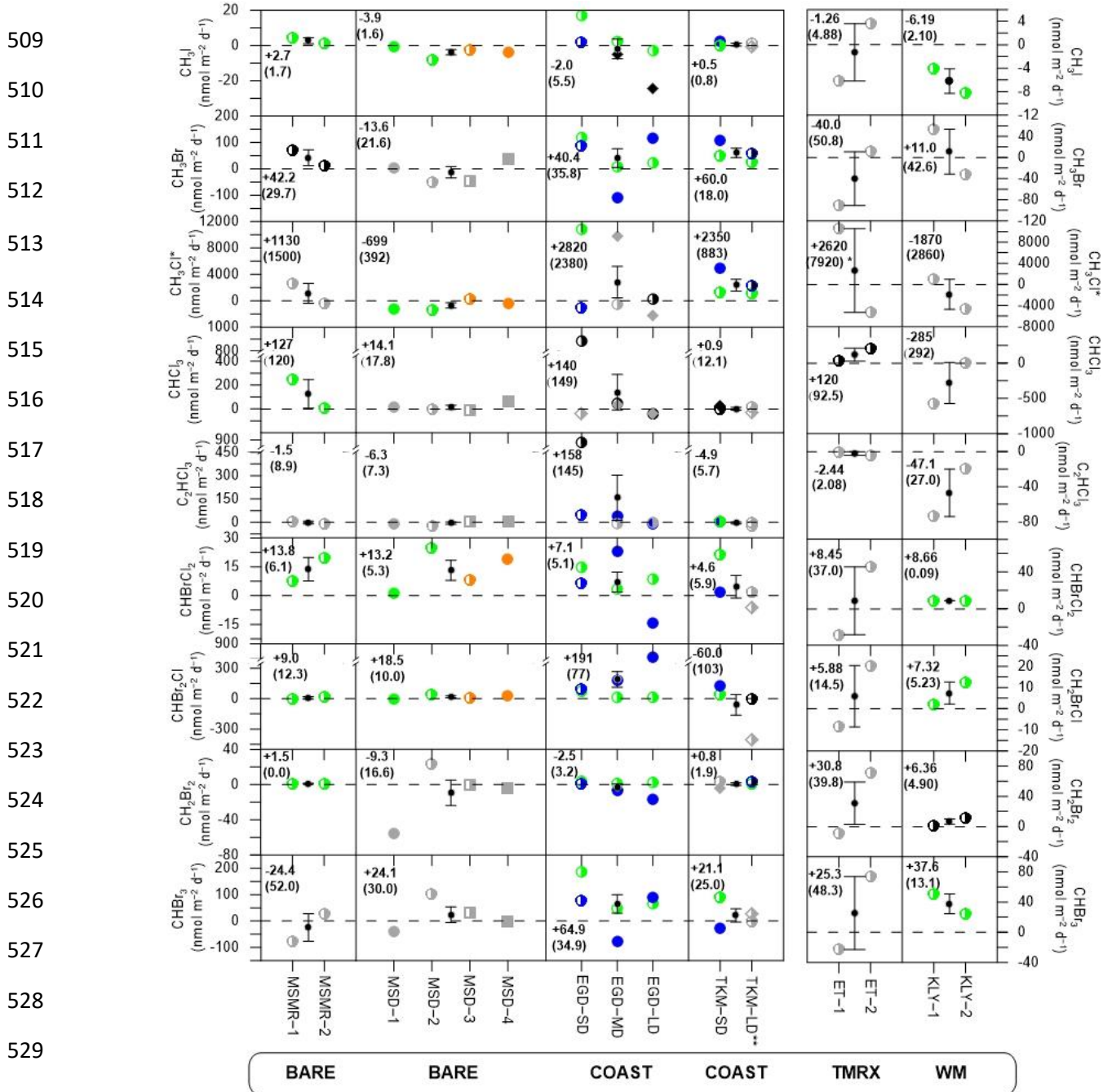
503 ^a $0.05 < p < 0.1$ for a measurement site as net source or sink for a specific species.

504 ^b $0.1 < p < 0.15$ for a measurement site as a net source or sink for a specific species; S and NS indicate $p < 0.05$ and
 505 $p > 0.05$, respectively.

506 * Flux calculation excludes one measurement for all VHOCs (see Sect. 2.1.2).

507 ** Flux calculation excludes one CH_3Cl sample (see Sect. 2.1.2).

508



530 $p\text{-val} < 0.05$ ● Spring ● Spring-prec. ● Winter ● Winter-prec. ● Summer ● Summer-eve.
 531 $0.05 < p\text{-val} < 0.1$ ● Spring ● Spring-prec. ● Winter ● Winter-prec. ● Summer ● Summer-eve.
 532 $p\text{-val} > 0.1$ ● Spring ● Spring-prec. ● Winter ● Winter-prec. ● Summer ● Summer-eve.

533 **Figure 3.** VHOC fluxes at the different measurement sites. Fluxes associated with p -values < 0.05 are marked by
 534 colored circles to indicate measurements during spring, winter, and summer, with full-colored circles indicating

535 measurements up to 3 days after a rain event in spring (Spring-prec.), up to 6 days after a rain event in winter
536 (Winter-prec.) and in the evening in summer (Summer-eve). Gray and black shapes indicate fluxes associated with
537 no clear statistical significance ($p > 0.1$ and $0.05 < p < 0.1$, respectively). At the center of each graph, the small
538 black circles and error bars represent the average and standard error of the mean (SEM), respectively, for each
539 measurement site. Dashed lines represent zero flux. In each box, the numbers indicate the mean flux and SEM (in
540 parentheses) for each site and species. Additional information is provided about measurement conditions (Tables 1
541 and S6), measurement abbreviations (Table 1) and statistical analysis (Table 2). *Calculation of CH_3Cl flux mean
542 and SEM excludes one sample at TMRX-ET-1 (see Sect. 2.1.2). **Calculation of mean flux and SEM excludes
543 one sampling canister at COAST-TKM-LD (see Sect. 2.1.2).

544

545 **3.2 Factors controlling VHOC flux**

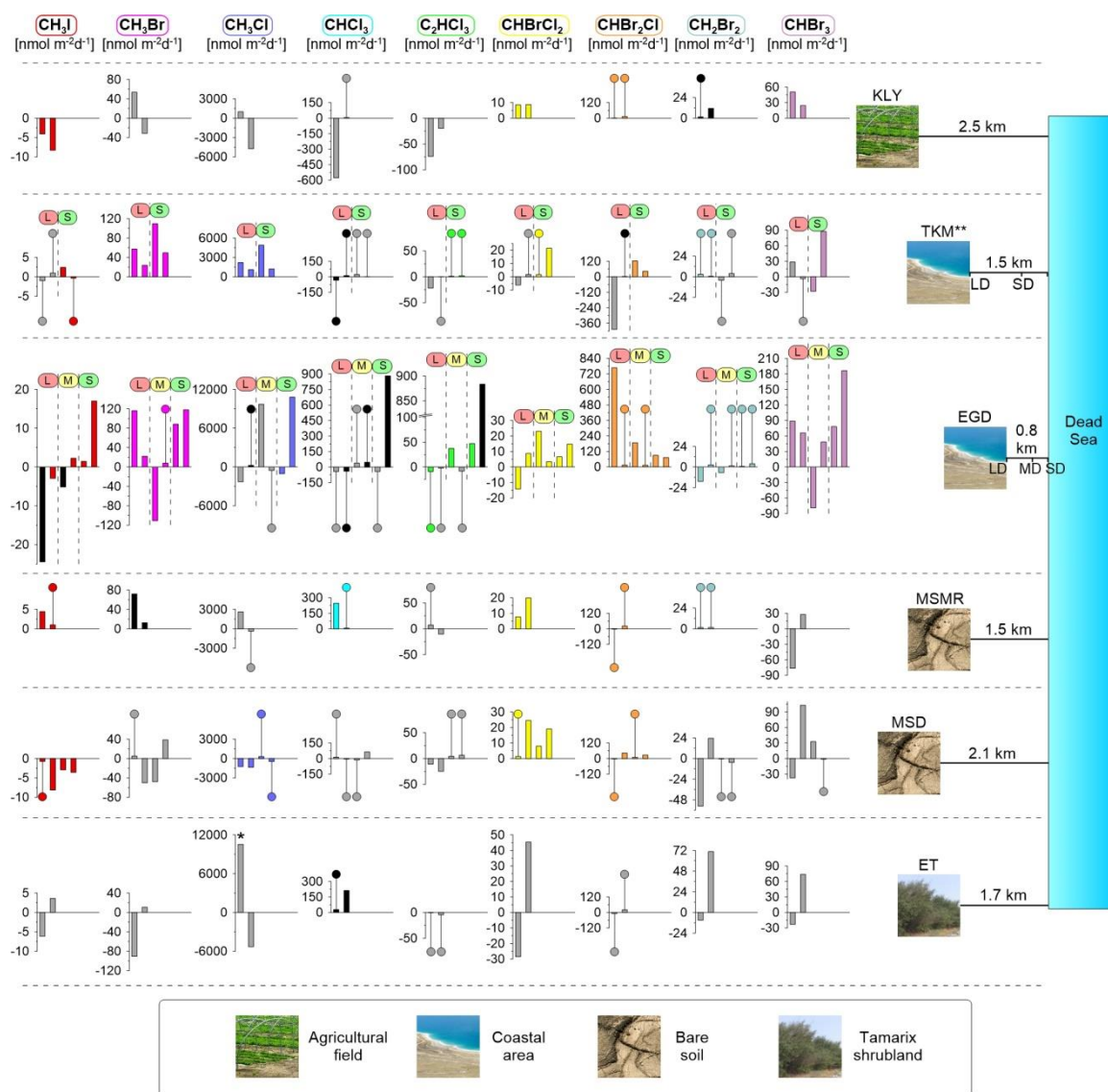
546 **3.2.1 Seasonal, meteorological and spatial effects**

547 The results presented in Sect. 3.1 showed elevated mixing ratios and net fluxes for all
548 investigated VHOCs, with relatively less frequent positive fluxes for CH_3I , CHCl_3 and C_2HCl_3 .
549 For all of the investigated VHOCs, a positive flux was measured for at least one of the two bare
550 soil sites, BARE-MSMR and BARE-MSD, which are located a few kilometers from the Dead
551 Sea water. For several VHOCs (CH_2Br_2 , CHBr_2Cl , CHBrCl_2 and CHCl_3), at least one of these
552 sites was identified as a significant net source ($p < 0.05$, Table 2). Additional measurements are
553 required to determine whether the other VHOCs are also emitted from these bare soil sites. Note
554 that for all VHOCs except C_2HCl_3 and CH_3Cl , measured mixing ratios were highest over at least
555 one of these bare soil sites (Table S3). Figure 4 further provides the spatial distribution of the
556 investigated VHOCs at the various sites. Elevated positive fluxes are seen at the coastal sites,
557 with a general tendency toward higher positive net fluxes closer to the seashore. Figure 4 also
558 demonstrates relatively high positive fluxes for the natural vegetation in TMRX-ET, higher than
559 for WM-KLY. However, additional measurements are required to decipher whether this site can
560 be classified as a statistically significant source for VHOCs (see Table 2).

561 No clear impact of meteorological conditions on the measured net flux rates or mixing ratios
562 was observed. We could not identify any clear association between flux magnitude and any

563 parameter, including solar radiation intensity, measurement time, temperature, and daytime
 564 relative humidity.

565



566

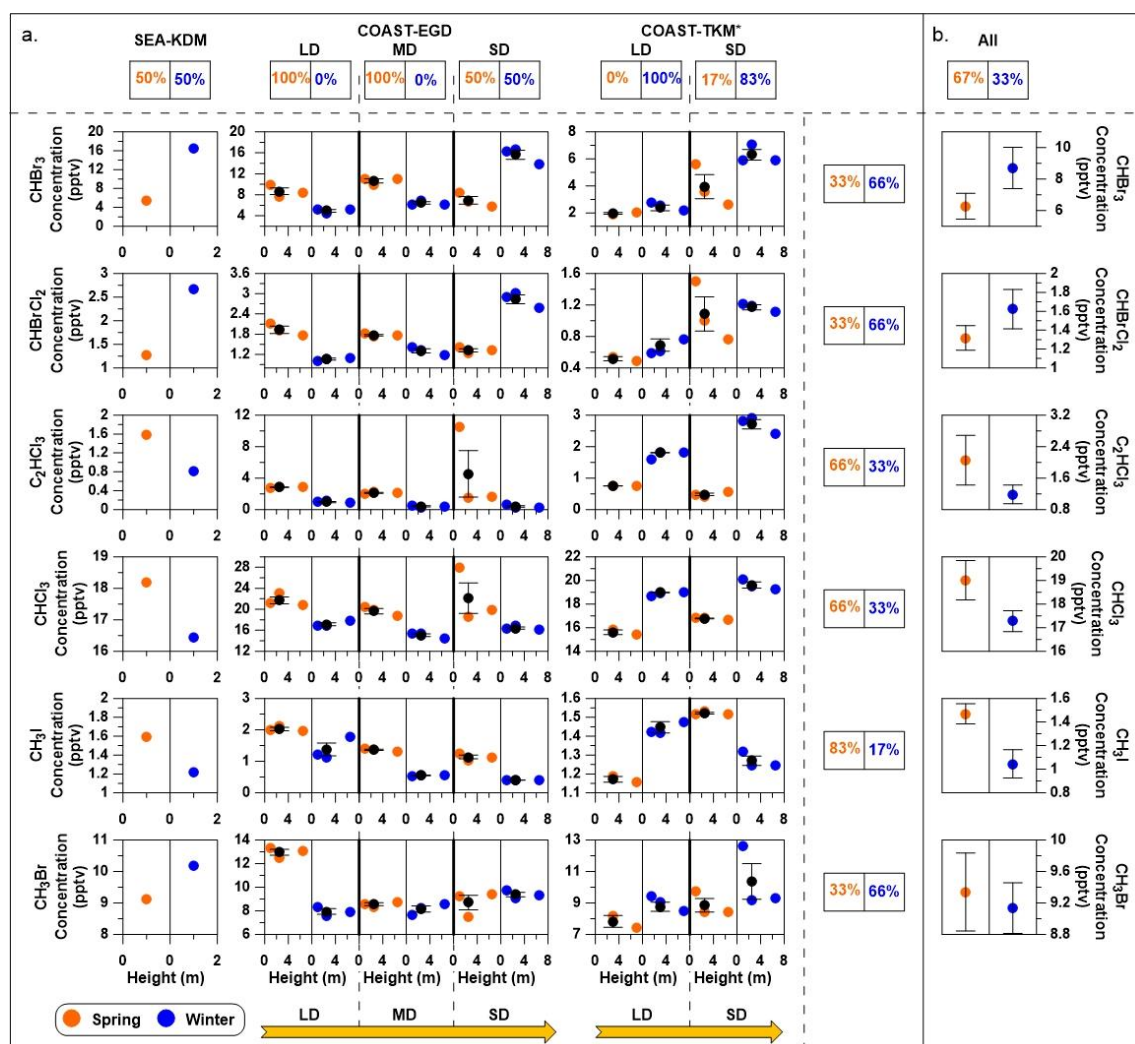
567 **Figure 4.** Bar graphs of VHOc fluxes from the different site types, organized by relative orientation to the Dead
 568 Sea and with visual indicators of surface cover type. Colored bars represent measured fluxes associated with *p*-
 569 values < 0.05. Gray and black bars indicate fluxes associated with no clear statistical significance (black for 0.05 < *p*
 570 < 0.1 and gray for *p* > 0.1). Circles with drop lines are used to mark fluxes with relatively low values. Different
 571 colors refer to different VHOcs as indicated at the top of the figure. The different site types are indicated in the
 572 legend. S, M and L indicate short, medium and long distance of the measurement site from the seawater for the
 573 coastal sites (SD, MD and LD, respectively; see Sect. 2.1.1). See Table 1 for measurement sites and measurement
 574 abbreviations. *CH₃Cl flux calculation excludes one sample in TMRX-ET-1 (see Sect. 2.1.2). **Flux calculation
 575 excludes one sampling canister in COAST-TKM-LD (see Sect. 2.1.2).

576 Our findings on the effects of season and distance from the sea on the measured fluxes are
577 presented in Fig. 3, which shows the measured fluxes for spring and winter and for different
578 distances from the sea at COAST-EGD and COAST-TKM. Differences in VHOC emissions
579 between winter and spring may arise from the generally much higher temperature, and lower
580 precipitation during the latter; further considering the high evaporation rate in this area, the soil
581 water content is expected to be generally lower in spring compared to winter (Sect. 2.1.1; see
582 also Table S6). Figure 3 suggests that there were no clear differences in VHOC fluxes between
583 spring and winter, as supported by statistical analysis, except for CH₃I and CH₂Br₂ for which
584 fluxes were higher in the spring, with moderate statistical significance ($0.05 < p < 0.1$).

585 No clear impact of distance from the seawater on the measured net fluxes could be detected,
586 including in cases where a significant fraction of the footprint included the seawater, such as for
587 COAST-EGD-SD-w and COAST-EGD-SD-s. However, owing to variations in soil properties,
588 the emissions near the seawater tended to be more frequent and more intense (see Sects. 3.2.2,
589 3.2.3).

590 Figure 5 compares the mixing ratios of the measured VHOCs at different distances from the
591 seawater, individually for winter and spring. Note that differences in sampling heights at
592 different sites can lead to a biased comparison between mixing ratios at different sites;
593 nevertheless, in most cases, differences across measurement sites were larger than across
594 vertical heights. No clear impact of season or distance from the seawater on the mixing ratios
595 can be discerned in this figure, also based on the sampling over SEA-KDM which directly
596 represents air masses over the seawater (Sect. 2.1.1). Nevertheless, further investigation, using
597 direct flux measurements over the Dead Sea water, is needed to study the potential emission of
598 VHOCs from this water body. While no clear impact of season on mixing ratios was observed,
599 for most sites, differences between two measurement sets resulted in consistent differences in
600 mixing ratios, such that one measurement set resulted in higher mixing ratios for all or most
601 species than the other. This suggests that other factors play a significant role in emission rates of

602 all or most VHOCs in the studied area. Only the CH₃I results indicated moderate statistical
 603 significance ($0.05 < p < 0.1$) for higher mixing ratios in the spring vs. winter, in agreement with
 604 seasonal trends for its flux, as discussed above.



605 **Figure 5.** Seasonal and spatial influences on measured mixing ratios of VHOCs for coastal sites only. (a)
 606 Measured VHOC mixing ratios are presented vs. vertical height above surface level, separately for winter (blue)
 607 and spring (orange). Black filled circles and error bars represent average and SEM, respectively. LD, MD and SD
 608 indicate long, medium and short distance from the seawater, respectively, while SEA-KDM is located at the
 609 seawater (see Sect. 2.1.1). Values above and to the right of the figure indicate the percentages of higher average
 610 mixing ratios in spring (left box) or winter (right box), individually for each site (SEA-KDM, COAST-TKM and
 611 EGD sites) and for SEA-KDM, COAST-EGD and COAST-TKM sites) and for each specific species, respectively. (b) For each species,
 612 the average mixing ratios over all sites (SEA-KDM, COAST-EGD and COAST-TKM) are presented (All), and the corresponding percentage of higher
 613 average mixing ratios in spring and in winter are also presented. See Table 1 for measurement site abbreviations.
 614 Species with no observed difference between seasons were excluded (see Fig. S1 for complete information); y axes

615 for sites in the same coastal area (COAST-TKM or COAST-EGD) are evenly scaled. *Measurements exclude one
616 sampling canister at COAST-TKM-LD (see Sect. 2.1.2).

617

618 **3.2.2 Impact of specific site characteristics and ambient conditions**

619 The formation of VHOCs requires a chemical interaction between OM and halides, induced by
620 biogeochemical, biochemical, or macrobiotic processes (Kotte et al., 2012; Breider and Albers,
621 2015). Despite the extreme salinity, biotic activity was detected in both the water and the soil of
622 the Dead Sea (see Sect. 1), demonstrating that biotic activity can potentially contribute to
623 VHOC emission in this area. Previous studies on emission of VHOCs from soil and sediments
624 revealed that OM content and type, halide ion concentrations, pH, and the presence of an
625 oxidizing agent (most frequently referred to as Fe(III)) also play important roles in the emission
626 rate of VHOCs (see (Kotte et al., 2012)).

627 Table 3 provides a basic representation of the soil composition parameters. The results
628 presented in Table 3 show substantial enrichment of Cl and Br in the sites closest to the
629 seawater (COAST-EGD-SD and COAST-TKM-SD) and lower concentrations at greater
630 distances from the seawater. For comparison, both Br and Cl concentrations were generally
631 much higher than those reported by Kotte et al. (2012) for various saline soils and sediments
632 (0.12–0.32 g kg⁻¹ and 6.1–120 g kg⁻¹, respectively), but lower for Br at BARE-MSMR and
633 BARE-MSD and for both Cl and Br at WM-KLY. No enrichment of I in the soil samples was
634 observed (e.g., see Keppler et al. (2000); Kotte et al. (2012)). The OM content of the samples
635 was generally higher than would be expected in desert soil. For comparison, forest floors
636 typically contain 1–5% OM (Osman, 2013). Detection of VHOC emissions from the soil is, in
637 some cases, associated with higher soil OM (e.g., Albers et al., 2017; Keppler et al., 2000) and in
638 some cases with lower soil OM (e.g., Kotte et al., 2012; Hubber et al., 2009) than that reported
639 here. Table 3 provides only a lower limit of the total Fe, rather than Fe(III), in the samples.
640 Note, however, that soil Fe content similar to that reported here as a low-limit value corresponds
641 with those associated with the finding of small amounts of VHOC emissions, while the emission

642 rates become saturated when enrichment with Fe(III) is relatively minor (Keppler et al., 2000).
643 Saturation at relatively low soil Fe concentrations was also reported by Huber et al. (2009).
644 Hence, variations in Fe across different sites may play a minor role in affecting emission rates.

645 While the number of samples collected at each site was limited, Table 2 and Fig. 4 indicate
646 elevated positive fluxes for the SD sites, and to some extent also at COAST-EGD-MD, with
647 respect to both statistically significant and non-statistically significant positive fluxes.
648 Moreover, for both COAST-EGD and COAST-TKM, during both spring and winter, the
649 occurrence of positive fluxes was correlated with proximity to seawater (i.e., COAST-EGD-SD
650 > COAST-EGD-MD > COAST-EGD-LD, and COAST-TKM-SD > COAST-TKM-LD). All
651 of these COAST sites contain mixtures of soil and salt-deposited structures (see Sect. 2.1.1), and
652 Table 3 indicates that soil concentrations of both Br and Cl correlated with proximity to
653 seawater at both COAST-EGD and COAST-TKM. The concentration of I in the soil showed a
654 similar trend only at the COAST-TKM sites (see Table 3). The association between the
655 magnitude and incidence of the positive net flux and soil halide concentrations points to an
656 increase in VHOC emission with salinity, even under the hypersaline conditions of the Dead Sea
657 area. This interpretation is supported by the fact that whereas for COAST-TKM-SD, both soil
658 water and OM content were relatively high, for COAST-EGD-SD, no other measured
659 parameter which could limit the emission of VHOCs, except for the soil halide concentration,
660 was higher than for both COAST-EGD-MD and COAST-EGD-LD (Table 3). The fact that
661 emission rates for COAST-TKM tended to be similar or lower in terms of incidence and
662 magnitude compared to COAST-EGD (Table 2) suggests, in view of the apparently lower Fe
663 content for the latter (Table 3), that the emission of VHOCs from these sites is not significantly
664 limited by the availability of Fe(III) in the soil.

665 COAST-EGD-SD-s was associated with the highest incidence of both statistically
666 significant and non-significant positive fluxes. Fluxes at COAST-EGD-SD-w were generally
667 lower and with a smaller incidence of positive fluxes. Based on the wind direction, in both

668 cases, the sampling footprint included both the seawater and a narrow strip of bare soil mixed
669 with salty beds (estimated at about 60% of the footprint) very close to the seawater. The main
670 notable difference between the two measurement days was that precipitation occurred just
671 before the COAST-EGD-SD-w measurement, whereas there was no precipitation event for
672 several weeks prior to the COAST-EGD-SD-s measurement (Table 1). Rain events also
673 occurred ~1.5 and ~2.5 days before BARE-MSD-1 and BARE-MSD-2 measurements,
674 respectively. Note that the emission fluxes for BARE-MSD-1 were lower and more negative for
675 most of the species than those for BARE-MSD-3 or BARE-MSD-4. In addition, the occurrence
676 of positive net fluxes tended to increase according to the order BARE-MSD-1 < BARE-MSD-2
677 < BARE-MSD-3 (see Table 2). The analyses for both COAST-EGD and BARE-MSD suggest
678 that increased soil water content caused by rain events can decrease the emission rates or
679 enhance soil-uptake rates of certain VHOCs.

680 A reduction in net flux rates following rain events did not occur for all species, and was not
681 clearly consistent across the BARE-MSD and COAST-EGD-SD sites. Thus, further research
682 on the effects of rain on the various VHOCs and ambient conditions is required. Nevertheless,
683 the analyses clearly demonstrate that strong emission rates do not depend on rain occurrence, in
684 agreement with findings by Kotte et al. (2012). The lower emission fluxes following the rain
685 event may be attributable to the low infiltration rate of VHOCs into the soil, or to salt dilution
686 and washout, or both.

687 Our measurements suggested elevated contribution of natural vegetation to some of the
688 investigated VHOCs (Fig. 4), but with no statistical significance for this site being a source of
689 any of the investigated VHOCs (Table 2). This might reflect the fact that only a few
690 measurements are available for this site. No clear contribution of the agricultural vegetation to
691 the emission fluxes was found in this study.

693 **Table 3.** Soil properties – OM, soil water content (SWC), I, Br, Cl and Fe fraction of dry weight and pH. Analyses
 694 were performed for a single mixture of samples at each site. See Table 1 for measurement site abbreviations.

Site	pH	OM (%)	SWC (%)	I mg kg soil dw ⁻¹	Br g kg soil dw ⁻¹	Cl g kg soil dw ⁻¹	Fe mg kg soil dw ⁻¹
BARE–MSMR	7.46	1.96	1.90	2.24	0.007	6.70	>20800
BARE–MSD	7.41	3.61	3.61	2.79	0.027	41.2	>7450
COAST–EGD–SD	7.61	2.28	1.79	0.24	1.47	202	>1120
COAST–EGD–MD	7.93	0.35	0.35	0.57	0.293	37.4	>3140
COAST–EGD–LD	7.70	3.67	2.58	1.03	0.008	26.1	>5950
COAST–TKM–SD	7.43	24.1	33.7	3.19	3.93	169	>12500
COAST–TKM–LD	7.80	3.40	1.64	1.14	0.186	19.5	>10600
TMRX–ET	7.88	3.14	2.97	2.69	0.474	85.2	>10100
WM–KLY	7.64	4.10	1.40	1.69	0.013	1.12	>7680

695

696 **3.2.3 Factors controlling the flux of specific VHOCs**

697

698 *Trihalomethanes*: Differently than previous studies, brominated VHOCs had relatively higher
 699 overall incidence of positive fluxes than chlorinated VHOCs (Table 2). The overall average net
 700 flux of trihalomethanes decreased according to $\text{CHBr}_2\text{Cl} > \text{CHCl}_3 > \text{CHBr}_3 > \text{CHBrCl}_2$, while
 701 CHCl_3 showed the lowest incidence of positive and highest mean positive fluxes among all
 702 trihalomethanes.

703 Natural emission of trihalomethanes from soil has been shown to occur without microbial
 704 activity, induced via oxidation of OM by an electron acceptor such as Fe(III) (Huber et al.,
 705 2009) or via hydrolysis of trihaloacetyl compounds (Albers et al., 2017). The soils studied by
 706 Albers et al. (2017) were significantly richer in OM than the soils at the Dead Sea, except for
 707 COAST–TKM–SD. Hence, the apparently higher emission from the Dead Sea soil may indicate
 708 either a different mechanism leading to the release of trihalomethanes from the soil or only a
 709 weak dependency on availability of soil OM. The latter explanation may be supported by the
 710 fact that Albers et al. (2017) did not find any correlation between CHCl_3 emission rate and

711 organic Cl in the soil. Furthermore, our study points to higher emission rates and incidence of
712 VHOCs, and generally also of trihalomethanes, closer to the seawater (COAST-EGD and
713 COAST-TKM sites), which suggests higher sensitivity to soil halide content than OM (Sect
714 3.2.2).

715 While trihalomethane formation via OM oxidation has been reported to occur more rapidly
716 at low pH, and specifically at $\text{pH} < \sim 3.5$ (Huber et al., 2009; Ruecker et al., 2014), its formation
717 via hydrolysis of trihaloacetyl is expected to occur more rapidly at the relatively high pH of ≥ 7
718 (Hoekstra et al., 1998; Albers et al., 2017). Yet, according to Ruecker et al. (2014), in
719 hypersaline sediments, the formation of VHOCs via OM oxidation involving Fe(III) can occur
720 at $\text{pH} > 8$ for biotic processes. Therefore, given the relatively high pH (~ 7.4 – 7.9 , Table 3) at the
721 SD sites, as well as the BARE and WM-KLY sites, the high trihalomethane-emission rates from
722 both bare and agricultural field sites support the work by Albers et al. (2017) concerning the
723 emission of trihalomethanes from the soil following trihaloacetyl hydrolysis.

724 Albers et al. (2017) showed that their proposed mechanism supports the emission of
725 CHCl_3 and CHBrCl_2 from soil, and suggested that additional halomethanes with a higher
726 number of Br atoms can be expected to be emitted via this mechanism, but at much lower rates.
727 Hence, the elevated net fluxes for CHBr_2Cl and CHBr_3 at the Dead Sea (Table 2) could occur
728 either because of the markedly higher composition of Br in the Dead Sea soil (see Table 3) or
729 because another mechanism is also playing a role in the emission; note that agriculture could
730 potentially be a source for the emission of CHBr_2Cl and CHBr_3 for WM-KLY, but not for the
731 other sites (Sect. 2.1.1). Hoekstra et al. (1998) finding that Br enrichment mainly enhances the
732 emission of CHBr_3 and CHBr_2Cl , rather than that of CHBrCl_2 , supports the former possibility,
733 namely, relatively elevated emission of CHBr_2Cl and CHBr_3 due to higher Br content in the soil.
734 While both Cl and Br soil contents are relatively high for both COAST SD sites and COAST-
735 EGD-MD, where emission of brominated trihalomethanes was higher than that of chlorinated
736 trihalomethanes (see Table 2), a remarkably high Br/Cl value (1:43) relative to other sites was

737 found at COAST-TKM-SD. Table 2 does not indicate a clear difference in the flux magnitude
738 of the brominated compared to chlorinated trihalomethanes for this site, suggesting that the main
739 reason for the relatively elevated brominated trihaloethanes at the SD sites and COAST-EGD-
740 MD is the high Br content rather than the Br/Cl ratio.

741 The relatively elevated net flux of brominated trihalomethanes from BARE and WM-KLY
742 indicates that relatively high rates of emission of these species can also occur from soils that are
743 much less rich in Br than the SD sites and COAST-EGD-MD site (see Tables 2, 3). Yet, the
744 emission rates of CHBrCl_2 at the Dead Sea were generally higher than those observed by Albers
745 et al. (2017), probably reflecting the higher soil Cl content at the Dead Sea.

746 *Methyl halides:* A relatively high incidence of negative fluxes was observed for CH_3Br ,
747 and more statistically significantly so for CH_3Cl and CH_3I , implying high rates of both emission
748 and deposition, at least for the latter two, in the studied area (Table 2). The average positive flux
749 of CH_3Cl was the highest of all VHOCs investigated, indicating strong emission and deposition
750 for this species at the Dead Sea. Several studies have indicated that soil tends to act as a sink for
751 CH_3Cl (Rhew et al., 2003). The relatively high positive net fluxes of CH_3Cl and CH_3Br at
752 WM-KLY-1 (983 and $53.5 \text{ nmol m}^{-2} \text{ d}^{-1}$, respectively) may point to emission of this species
753 from the local agricultural field, in agreement with previous studies (Sect. 1), potentially by
754 microbial- or fungal-induced emission (Moore et al., 2005; Watling and Harper, 1998), but this
755 should be further investigated considering the lack of statistical significance.

756 Positive net fluxes for CH_3I were not significantly higher than those obtained in previous
757 studies (Sect. 3.1), a finding that might be attributed to the small concentration of I in the soil
758 relative to those of the other halides. At Duke Forest, Sive et al. (2007) observed a soil-emission
759 CH_3I flux of $\sim 0.27 \text{ nmol m}^{-2} \text{ d}^{-1}$ on average (ranging from ~ 0.11 to $0.31 \text{ nmol m}^{-2} \text{ d}^{-1}$) under
760 precipitation conditions in June, and higher emission rates (0.8 and $4.1 \text{ nmol m}^{-2} \text{ d}^{-1}$) under
761 warmer and dryer conditions in September. In agreement with those findings, although in
762 general our analyses did not indicate clear seasonal effects, we found that in all cases, net CH_3I

763 fluxes were higher in spring than in winter, except for COAST-TKM-SD (Fig. 3). As discussed
764 in Sect. 3.2.1, the mixing ratios of CH₃I also tended to be higher in magnitude in spring
765 compared to winter, with moderate statistical significance ($0.05 < p < 0.1$ in both cases) (Figs. 3,
766 5).

767 Relatively high fluxes of CH₃Cl and CH₃Br, and to a lesser extent of CH₃I, were observed at
768 the COAST-TKM and COAST-EGD sites, particularly from the sites closest to the seawater
769 (Fig. 4). According to Keppler et al. (2000), the presence of Fe(III), OM and halide ions is
770 basically sufficient to result in emission of methyl halides from both soil and sediments by a
771 natural abiotic process (Sect. 1). The strong emission of methyl halide from the COAST-TKM
772 and COAST-EGD sites indicates that these species can be emitted at high rates from saline soil
773 that is not rich in OM. The strongest emissions occurred from COAST-TKM-SD and
774 COAST-EGD-SD, which may indicate high sensitivity of methyl halide emission to soil OM
775 and/or halide content (see Table 3). The fact that the emission of methyl halides, particularly
776 CH₃Br and CH₃Cl, from COAST-TKM-SD, where soil OM is substantially higher than at all
777 other investigated sites, was not higher than the emission from COAST-EGD-SD-s may
778 indicate that emission of methyl halides was not sensitive to soil OM in our study. Note that the
779 lower fluxes for EGD-SD-w compared to EGD-SD-s can be associated to a prior rain event for
780 the former (Sect. 3.2.2).

781 In controlled experiments to study emissions of the three methyl halides from soil, Keppler
782 et al. (2000) found a decrease in the efficiency of methyl halide emission according to CH₃I >
783 CH₃Br > CH₃Cl (10:1.5:1; mole fractions). We estimated the emission efficiencies of the
784 different methyl halides based on the ratio between their fluxes and the concentrations of halide
785 in the soil. To maintain consistency with the calculations of Keppler et al. (2000), our
786 calculation was also based on mole fractions, and took into account only positive fluxes, on the
787 assumption that they are closer in magnitude to emission. This corresponded with measured soil
788 halide concentration proportions for Cl:Br:I of 2.4E5:1.5E3:1, and the evaluated emission

789 efficiency proportions were 15:1.4:1 for CH₃I, CH₃Br and CH₃Cl, respectively, when two
790 outliers were excluded from the calculations. These calculations confirmed the increasing
791 efficiency of methyl halide emission following: CH₃Cl < CH₃Br < CH₃I, in agreement with
792 Keppler et al. (2000), suggesting that at least the methylation and emission of CH₃Br and CH₃Cl
793 in our study were controlled by abiotic mechanisms similar to those reported by Keppler et al.
794 (2000). The apparently higher relative efficiency of CH₃I emission may indicate emissions of
795 CH₃I via other mechanisms in the studied area, as discussed in Sect. 3.3. It should be noted,
796 however, that the fluxes that we used for the methyl halide emission efficiencies were based on
797 measured net flux rather than measured emission flux. This might also explain the inconsistency
798 between the relative CH₃I-emission efficiency calculated by Keppler et al. (2000) and by us.

799 C₂HCl₃: C₂HCl₃ had the second lowest incidence of positive fluxes, with statistically
800 significant ($p < 0.05$) positive fluxes only from the COAST SD sites and COAST-EGD-MD
801 (Table 2). These sites are mixtures of salt beds and deposits with salty soil and therefore, the
802 elevated emissions of C₂HCl₃ at these sites appear to support previous evidence for the emission
803 of this gas by halobacteria from salt lakes, as reported by Weissflog et al. (2005). Additional
804 chlorinated VHOCs, including CHCl₃ and CH₃Cl, also demonstrated increased emission from
805 this site, in line with the findings of Weissflog et al. (2005). Note that the net measured fluxes
806 for most of the VHOCs investigated at the COAST-EGD-SD-w site were smaller than those at
807 COAST-EGD-SD-s, as discussed in Sect. 3.2.2.

808 CH₂Br₂: CH₂Br₂ showed positive fluxes from all site types, with a positive average net
809 flux from most sites (see Fig. 3), but its fluxes over the vegetated and agricultural sites were not
810 statistically significant. Correlation of CH₂Br₂ with trihalomethanes will be discussed in Sect.
811 3.3.

812 3.3 Flux and mixing ratio correlations between VHOCs

813 Table 4 presents the Pearson correlation coefficients (r) between the measured mixing ratios of
814 VHOCs at the Dead Sea, separately for all sites and for the terrestrial sites only, as well as
815 separately for BARE, COAST, and the natural vegetation and agricultural field sites (VEG). For
816 COAST, r is also presented individually for the two sites which were closest to the seawater
817 (SD). The correlations' significance levels are also indicated. In most cases, the correlations
818 between species over all terrestrial sites were low, but were substantially higher for the
819 brominated trihalomethanes [CHBr_3 – CHBrCl_2 ($r = 0.79$), CHBr_2Cl – CHBrCl_2 ($r = 0.87$), and
820 CHBr_2Cl – CHBr_3 ($r = 0.85$)], supporting a common source mechanism for these species. High
821 correlations between these three trihalomethanes can be attributed to high correlations at the
822 BARE and VEG sites. Relatively high correlations were also obtained, although to a lesser
823 extent, between methyl halides, particularly between CH_3Cl and CH_3Br ($r = 0.75$), which can be
824 attributed to correlations at the COAST sites, particularly the SD sites. For COAST, and
825 particularly for SD, a high correlation was observed between C_2HCl_3 and CHCl_3 . Correlations
826 were in most cases either similar or smaller when we included measurements from the seawater
827 site SEA–KDM, which may reinforce the notion that emission from the seawater does not
828 contribute significantly to VHOC mixing ratios in the area of the Dead Sea.

829 **Table 4.** Correlations between the mixing ratios of VHOCs. Shown is the Pearson correlation coefficient (*r*)
830 between each VHOC pair for the measured mixing ratio, when calculated over all sites excluding SEA-KDM (NO-
831 KDM), all sites (ALL), bare soil sites (BARE), coastal sites (COAST), short distance from the sea at the coastal
832 sites (SD) and the vegetated sites (VEG). Correlations were calculated for mean mixing ratios at each site. The *p*-
833 value for *r* being significantly different from zero is indicated based on one-sample t-test, in four categories: value
834 in bold, *p* < 0.05; value in parentheses, *p* > 0.15; ^a*p* < 0.1; ^b*p* < 0.15.

		CHBrCl ₂	CHBr ₃	CHBr ₂ Cl	CHCl ₃	CH ₂ Br ₂	C ₂ HCl ₃	CH ₃ Cl	CH ₃ Br
CH ₃ I	NO-KDM (n=20)	(-0.23)	(-0.15)	(-0.15)	0.45	(0.12)	(0.17)	(0.31)	0.36
	ALL (n=22)	(-0.23)	(-0.15)	(-0.15)	0.45	(0.10)	(0.16)	(0.31)	0.36 ^a
	BARE (n = 6)	0.76 ^b	0.90 ^a	0.84 ^a	(0.32)	(-0.12)	(0.18)	(0.38)	(0.34)
	COAST (n = 10)*	0.78	(0.39)	(0.57)	(0.42)	(0.24)	(0.29)	0.86	(0.55)
	SD (n = 4)	-0.95	(0.21)	(0.14)	(-0.23)	(-0.06)	(-0.41)	(0.60)	(0.63)
	VEG (n = 4)	(-0.49)	(-0.45)	(-0.51)	0.86 ^b	(0.79)	(-0.11)	0.85 ^b	(0.62)
CH ₃ Br	NO-KDM	(0.19)	0.37 ^b	(0.26)	0.43	0.52	(0.19)	0.75	
	ALL	(0.18)	0.38 ^b	(0.25)	0.42	0.51	(0.17)	0.75	
	BARE (n = 6)	(0.00)	(0.01)	(-0.05)	(0.49)	0.98	(0.08)	(0.38)	
	COAST (n = 10)*	(0.22)	(0.60)	(0.46)	(0.54)	(0.32)	(0.39)	0.86	
	SD (n = 4)	(-0.58)	0.88 ^a	(0.77)	(0.56)	(0.41)	(0.41)	0.99	
	VEG (n = 4)	(0.27)	(0.30)	(0.22)	(0.76)	0.93 ^a	(-0.73)	(0.78)	
CH ₃ Cl**	NO-KDM	(0.04)	(0.21)	(0.13)	0.53	(0.08)	(0.12)		
	ALL	(0.00)	(0.04)	(0.02)	0.28	0.01	0.12		
	BARE (n = 6)	(0.39)	(0.71)	(0.53)	(0.70)	(0.29)	(0.18)		
	COAST (n = 10)*	(0.39)	(0.50)	(0.45)	(0.36)	(0.21)	(0.29)		
	SD (n = 4)	(-0.51)	0.91 ^a	(0.71)	(0.63)	(0.30)	(0.47)		
	VEG (n = 4)	(-0.39)	(-0.35)	(-0.44)	1.00	0.95	(-0.59)		
C ₂ HCl ₃	NO-KDM	(0.11)	(0.18)	(0.16)	(0.26)	(-0.01)			
	ALL	(0.12)	(0.09)	(0.17)	0.27	0.00			
	BARE (n = 6)	(0.78)	(0.56)	(0.75)	(0.63)	(-0.12)			
	COAST (n = 10)*	(0.39)	(0.50)	(0.38)	0.93	(0.24)			
	SD (n = 4)	(0.50)	(0.79)	(0.56)	0.98	(0.26)			
	VEG (n = 4)	(-0.30)	(-0.32)	(-0.25)	(-0.56)	(-0.70)			
CH ₂ Br ₂	NO-KDM	(0.06)	(0.23)	(0.12)	(0.17)				
	ALL	(0.07)	(0.20)	(0.12)	(0.17)				
	BARE (n = 6)	(-0.19)	(-0.13)	(-0.24)	(0.32)				
	COAST (n = 10)*	(0.67)	(0.77)	(0.52)	(0.42)				
	SD (n = 4)	(-0.18)	(0.41)	0.87 ^b	(0.26)				
	VEG (n = 4)	(-0.10)	(-0.06)	(-0.15)	0.95				
CHCl ₃	NO-KDM	0.35 ^b	(0.27)	(0.24)					
	ALL	(0.35)	(0.21)	(0.24)					
	BARE (n = 6)	0.84 ^a	0.77 ^b	0.84 ^a					
	COAST (n = 10)*	(0.51)	(0.59)	(0.57)					
	SD (n = 4)	(0.34)	0.89 ^a	(0.63)					
	VEG (n = 4)	(-0.41)	(-0.38)	(-0.46)					
CHBr ₂ Cl	-NO-KDM	0.87	0.85						
	ALL	0.87	0.75						
	BARE (n = 6)	0.97	0.90						
	COAST (n = 10)*	(0.17)	(0.39)						
	SD (n = 4)	(-0.25)	(0.81)						
	VEG (n = 4)	1.00	1.00						
CHBr ₃	NO-KDM	0.79							
	ALL	0.69							
	BARE (n = 6)	0.76 ^b							
	COAST (n = 10)*	0.78 ^a							
	SD (n = 4)	(-0.13)							
	VEG (n = 4)	(0.76)							

835

836 * Correlation calculation for COAST-TKM-LD excluded one sampling canister (see Sect. 2.1.2).

837 ** Correlation calculation for CH₃Cl excluded one sample for TMRX-ET-1 (see Sect. 2.1.2).

838 Table 5 shows the correlations between the measured VHOC fluxes, separately for all sites,
839 BARE sites, VEG sites, TMRX-ET site and WM-KLY site, as well as for COAST-TKM and
840 COAST-EGD sites. For the latter two sites, correlations are also presented separately for the SD
841 sites. Note that the table compares net flux rather than emission flux, and therefore the reported
842 correlations are expected to be affected by both sinks and sources for the different VHOCs.

843 The results in Table 5 show moderate to high positive correlations in most cases when all
844 sites are included in the calculation, whereas in many cases, the correlations were significantly
845 higher when calculated for sites of the same type, suggesting common emission mechanisms or
846 controls. High correlations were obtained for VEG between CHBrCl_2 , CHBr_2Cl and CHBr_3 ($r \geq$
847 0.94 ; $p < 0.05$), except for the correlation between CHBr_2Cl and CHBr_3 ($r = 0.82$; $p > 0.15$).
848 Note that these correlations can potentially be attributed to agricultural emission, considering
849 that WM-KLY, but not TMRX-ET, was identified as a statistically significant source for the
850 three trihalomethanes. At the BARE sites, high positive correlations between the fluxes of the
851 three brominated trihalomethanes were observed which were all associated with p -values < 0.05 ,
852 except for a lower correlation between CHBr_3 and CHBrCl_2 ($r = 0.72$; $p < 0.1$). Furthermore,
853 high correlations between the mixing ratios of the three trihalomethanes were obtained for these
854 two sites, although relatively low statistical significance was obtained for the correlation
855 between CHBr_3 and CHBrCl_2 at these sites (see Table 4). This further supports the notion that
856 the three brominated trihalomethanes are emitted via similar mechanisms or controls.
857 Moderately low p -values for the correlations between CH_2Br_2 and both $\text{CH}_2\text{Br}_2\text{Cl}$ ($p < 0.15$) and
858 CHBrCl_2 ($p < 0.1$) at these sites further suggests common controls for CH_2Br_2 and the
859 brominated trihalomethanes (see Table 5).

860 Correlation of CH_2Br_2 with CHBr_2Cl at the SD sites was strongly negative ($r = -0.93$; $p <$
861 0.1), similar to the negative correlation between CHBr_2Cl and the other brominated
862 trihalomethanes, CHBrCl_2 ($r = -0.98$; $p < 0.05$) and CHBr_3 ($r = -0.65$; $p > 0.15$) at these sites.
863 This, together with the fact that the measured fluxes of these three species were generally

864 positive over the SD sites, suggest competitive emission between CHBr_2Cl and CHBrCl_2 and
865 potentially also CHBr_3 , at least at the SD sites. This is supported by the analysis in Sects. 3.2.2
866 and 3.2.3, which demonstrated that the halide content of the soil appears to play a major role in
867 controlling the emission rates of VHOCs under the studied conditions.

868 Table 5 also indicates overall low correlations between CHCl_3 and all of the brominated
869 trihalomethanes, mostly resulting from negative correlations at the BARE sites. The
870 anticorrelation of CHCl_3 with trihalomethanes increased in the order $\text{CHBrCl}_2 < \text{CHBr}_2\text{Cl} <$
871 CHBr_3 . The incidence of the chlorinated trihalomethanes (CHCl_3 and CHBrCl_2), compared to
872 the less chlorinated ones (CHBr_3 and CHBr_2Cl) also tended to be higher at the BARE sites
873 compared to the other sites (Table 2). Hence, the negative correlation between CHCl_3 and the
874 brominated trihalomethanes at the bare soil sites may indicate competitive emission between the
875 more chlorinated and more brominated trihalomethanes. The situation at the BARE sites
876 resembles previous reports of predominant emission of CHCl_3 at the expense of the more
877 brominated species (e.g., (Albers et al., 2017; Huber et al., 2009)), particularly CHBr_3 and
878 CHBr_2Cl , and was expected, given the higher Cl/Br ratio at these sites (see Table 3). We should
879 emphasize that even at the BARE sites, we observed relatively high positive fluxes of
880 brominated trihalomethanes, particularly CHBr_2Cl and CHBrCl_2 , which would not generally be
881 expected (Albers et al., 2017), and can be attributed to the relatively high Br enrichment in the
882 soil.

883 Interestingly, in agreement with Table 4, Table 5 also shows relatively high correlations
884 between CHCl_3 and all methyl halides, particularly for the BARE sites (CH_3I , $r = 0.68$, $p < 0.15$;
885 CH_3Br , $r = 0.83$, $p < 0.05$; CH_3Cl , $r = 0.86$, $p < 0.05$), and SD sites (CH_3I , $r = 0.99$, $p < 0.05$;
886 CH_3Br , $r = 0.59$, $p > 0.15$; CH_3Cl , $r = 0.91$, $p < 0.1$). Remarkably, a high correlation was found
887 for CH_3I with CHCl_3 and C_2HCl_3 at the SD sites ($r = 0.99$, $p < 0.05$ in both cases). Positive
888 fluxes of the three species were observed at the SD sites in most cases, although with only
889 moderate statistical significance for CHCl_3 (Table 2). Weissflog et al. (2005) found that

890 emission of C_2HCl_3 , $CHCl_3$ and other chlorinated VHOCs can occur from salt lakes via the
891 activity of halobacteria in the presence of dissolved Fe (III) and crystallized NaCl. The strong
892 correlations of $CHCl_3$, C_2HCl_3 and CH_3I at the SD sites, where statistically significant fluxes
893 were frequently measured for these species, reinforce the co-located emissions of $CHCl_3$ and
894 C_2HCl_3 from salt lake sediments, as indicated by Weissflog et al. (2005), and suggest that CH_3I
895 can be emitted in a similar fashion. The fact that the relative emission efficiency of CH_3I in our
896 study was much higher than under the conditions used by Keppler et al. (2000) supports the
897 possibility that mechanisms other than the abiotic emission pathway proposed by Keppler et al.
898 (2000) influence the emission of CH_3I at the Dead Sea (Sect. 3.2.3).

899 **Table 5.** Correlations between the measured net fluxes of VHOCs. The table records the Pearson
900 correlation coefficient (r) for the measured net flux between each VHOC pair, calculated over all sites except
901 SEA–KDM (All), bare soil sites (BARE), coastal sites (COAST), short distance from the sea at the coastal sites
902 (SD) and the vegetated sites (VEG). The *p*-value for r being significantly different from zero is indicated based on
903 *t*-test, in four categories: by default, bolded, *p* < 0.05; value in parentheses, *p* > 0.15; ^a*p* < 0.1; ^b*p* < 0.15.

		CHBrCl ₂	CHBr ₃	CHBr ₂ Cl	CHCl ₃	CH ₂ Br ₂	C ₂ HCl ₃	CH ₃ Cl	CH ₃ Br
CH ₃ I	All (n = 20)	0.34 ^b	(0.13)	-0.56	0.59	(0.19)	0.59	0.45	(0.23)
	BARE (n = 6)	(-0.54)	-0.85	-0.78	0.68 ^b	(-0.32)	(0.54)	0.73 ^a	0.77 ^a
	COAST (n = 10)*	0.50 ^b	(0.26)	-0.64	0.66	0.81	0.63	0.54 ^b	(0.08)
	SD (n = 4)	(0.13)	(0.72)	(-0.05)	0.99	(0.35)	0.99	0.90 ^b	(0.69)
	VEG (n = 4)	(0.76)	(0.72)	(0.57)	(0.31)	0.88 ^b	(0.16)	(0.11)	0.45
CH ₃ Br	All (n = 20)	(-0.08)	0.39 ^a	(0.22)	(0.20)	(-0.06)	0.33 ^c	(0.30)	
	BARE (n = 6)	(-0.22)	-0.83	(-0.45)	0.83	(-0.21)	(0.57)	(0.61)	
	COAST (n = 10)*	-0.51 ^a	0.65	(0.19)	(0.29)	(-0.04)	(0.33)	(-0.24)	
	SD (n = 4)	(-0.62)	(0.07)	(0.69)	(0.59)	(-0.40)	(0.59)	(0.69)	
	VEG (n = 4)	(0.67)	0.87 ^b	(0.47)	(-0.57)	(0.36)	(-0.76)	0.94	
CH ₃ Cl**	All (n = 19)	(0.27)	(0.05)	(0.00)	-0.37 ^b	(-0.15)	0.54		
	BARE (n = 6)	(-0.33)	(-0.63)	(-0.54)	0.86	(0.21)	0.71 ^b		
	COAST (n = 10)*	0.58 ^a	(-0.09)	(-0.16)	0.69	(0.14)	0.66		
	SD (n = 4)	(0.07)	(0.45)	(0.08)	0.91 ^a	(0.12)	0.86 ^b		
	VEG (n = 3)	(0.45)	(0.68)	(0.31)	(-0.75)	(0.06)	(-0.91)		
C ₂ HCl ₃	All (n = 20)	(0.10)	0.53	(0.05)	0.83	(0.02)			
	Bare (n = 6)	(-0.41)	-0.66 ^b	(-0.52)	(0.56)	(-0.10)			
	COAST (n = 10)*	(0.30)	0.65	(-0.01)	0.99	(0.26)			
	SD (n = 4)	(0.26)	(0.81)	(-0.19)	0.99	(0.48)			
	VEG (n = 4)	(-0.05)	(-0.34)	(0.12)	0.96	(0.33)			
CH ₂ Br ₂	All (n = 20)	0.62	0.36 ^b	(-0.17)	(0.15)				
	BARE (n = 6)	0.77 ^a	(0.58)	0.68 ^c	(0.08)				
	COAST (n = 10)*	(0.45)	(0.26)	-0.85	(0.27)				
	SD (n = 4)	0.90 ^a	0.88 ^c	-0.93 ^a	(0.45)				
	VEG (n = 4)	0.91 ^a	0.77 ^b	0.87 ^b	(0.55)				
CHCl ₃	All (n = 20)	(0.01)	(0.30)	(0.01)					
	BARE (n = 6)	(-0.25)	-0.74 ^a	(-0.46)					
	COAST (n = 10)*	(0.31)	0.60 ^a	(-0.04)					
	SD (n = 4)	(0.27)	(0.77)	(-0.18)					
	VEG (n = 4)	(0.22)	(-0.09)	(0.40)					
CHBr ₂ Cl	All (n = 20)	(-0.11)	(0.16)						
	Bare (n = 6)	0.95	0.86						
	COAST (n = 10)*	(-0.22)	(0.11)						
	SD (n = 4)	-0.98	(-0.65)						
	VEG (n = 4)	0.94	(0.82)						
CHBr ₃	All (n = 20)	(0.22)							
	BARE (n = 6)	0.72 ^a							
	COAST (n = 10)*	(-0.04)							
	SD (n = 4)	(0.65)							
	VEG (n = 4)	0.95							

904 * Correlation calculations for COAST–TKM-LD excluded one sampling canister (see Sect. 2.1.2).

905 ** Correlation calculation for CH₃Cl excluded one sample for TMRX–ET-1 (see Sect. 2.1.2).

906

907 **Summary**

908 The results of this study demonstrate high emission rates of the investigated VHOCs in the Dead
909 Sea region, corresponding with mixing ratios which, in most cases, are significantly higher than
910 typical values in the MBL. Overall, our measurements indicate a generally elevated incidence of
911 positive fluxes of brominated vs. chlorinated VHOCs compared to previous studies. The high
912 incidence of the former can be attributed primarily to the relatively large amount of Br in the
913 soil, rather than the Br/Cl ratio. We did not detect any clear effect of meteorological parameters,
914 emission from the seawater, or season, other than – in agreement with Sive et al. (2007) –
915 apparently higher emission of CH₃I in spring vs. winter. Three of the investigated site types –
916 bare soil, coast and agricultural field – were identified as statistically significant ($p < 0.05$)
917 sources for at least some of the investigated VHOCs. The fluxes, in general, were highly
918 variable, showing changes between sampling periods, even for a specific species at a specific
919 site. The coastal sites, particularly at a short distance from the sea (SD sites) where soil is mixed
920 with salt deposits, were sources for all of the investigated VHOCs, but not statistically
921 significantly for CHCl₃. Further from the coastal area, the bare soil sites were sources for
922 CHBrCl₂, CHBr₂Cl, CHCl₃, and apparently also for CH₂Br₂ and CH₃I, and the agricultural
923 vegetation site was a source for CHBr₃, CHBr₂Cl and CHBrCl₂. Our measurements reinforce
924 reports of CHCl₃ and CHBrCl₂ emission from bare soil, but indicate that such emission can also
925 occur under relatively low soil organic content. To the best of our knowledge, we report here for
926 the first time strong emission of CHBr₂Cl and emission of CH₂Br₂ from hypersaline bare soil, at
927 least a few kilometers from the Dead Sea. We could not identify the contribution of either
928 natural or agricultural vegetation to the emission of the investigated VHOCs.

929 The highest emissions from the SD sites were associated with maximum salinity, and clearly
930 showed an increased incidence of positive flux with proximity to the seawater, pointing to the
931 sensitivity of VHOC emission rates to salinity, even under hypersaline conditions. The
932 measurements did not indicate either increased or reduced emissions of VHOCs from the

933 seawater itself. Emission of VHOCs has been shown to occur from dry soil under semiarid
934 conditions during the summer, in agreement with the finding from other geographical locations
935 that soil water does not seem to be a limiting factor in VHOC emission (Kotte et al., 2012). Rain
936 events appeared to attenuate the emission rates of VHOCs at the Dead Sea. Measurements at a
937 bare soil site suggested a decrease in VHOC emission rates for 1–3 days after a rain event.

938 Both flux and mixing ratio correlation analyses pointed to common formation and
939 emission mechanisms for CHBr_2Cl and CHBrCl_2 , in line with previous studies, for the
940 agricultural watermelon-cultivation field and bare soil sites. These analyses further strongly
941 suggest common formation and emission mechanisms for CHBr_3 with these two
942 trihalomethanes. Whereas Albers et al. (2017) suggested that CHBr_3 and CHBr_2Cl are emitted
943 from soil only in relatively small amounts compared to CHCl_3 , our results indicated their high
944 emission via common mechanisms with the other trihalomethanes. The overall average net flux
945 of the trihalomethanes decreased according to $\text{CHBr}_2\text{Cl} > \text{CHCl}_3 > \text{CHBr}_3 > \text{CHBrCl}_2$, while
946 CHCl_3 showed the lowest incidence of positive fluxes among all trihalomethanes. The enhanced
947 emission of brominated trihalomethanes probably reflects enrichment of the Dead Sea soil with
948 Br, in line with findings by Hoekstra et al. (1998).

949 We identified the coastal sites as a probable source for all methyl halides, whereas neither
950 agricultural field nor natural vegetation site were identified as net sink or net source for these
951 species, except for the agricultural field being a net sink for CH_3I . Our analysis demonstrated,
952 however, much higher efficiencies of CH_3I emission than of CH_3Br and CH_3Cl emissions as a
953 function of halides in the soil, compared to those reported by Keppler et al. (2000), pointing to
954 emission of CH_3I via other mechanisms. The strong correlation between both fluxes and mixing
955 ratios of CH_3I , CHCl_3 and C_2HCl_3 , particularly at the SD sites, strongly suggests that the coastal
956 area of the Dead Sea acts as an emission source for CHCl_3 , C_2HCl_3 and CH_3I via similar
957 mechanisms, although these sites were associated with only moderate statistical significance ($p \leq$
958 0.1) as a net source for CHCl_3 . The emission of CHCl_3 and C_2HCl_3 from these sites is in line

959 with findings by Weissflog et al. (2005) of emission of various chlorinated VHOCs, including
960 CHCl_3 and C_2HCl_3 , from salt lake sediments. Weissflog et al. (2005) reported that the emission
961 of chlorinated VHOCs in their study was induced by microbial activity. Keppler et al. (2000)
962 reported the involvement of an abiotic process in the formation of alkyl from soil and sediments,
963 and the observed correlation between methyl halides and between CH_3I and both CHCl_3 and
964 C_2HCl_3 may indicate that the two processes occur simultaneously in the coastal area of the Dead
965 Sea.

966 Although relatively high, the CHBr_3 fluxes and mixing ratios that we measured at the
967 Dead Sea cannot be directly related to the high mixing ratios of reactive bromine species that
968 were found at the Dead Sea (e.g., see Matveev et al. (2001) and Tas et al. (2005)) via its
969 photolysis. Similarly, if CH_3I photolysis is the only source of reactive I species, the measured
970 fluxes and elevated mixing ratios of CH_3I are not high enough to account for the high iodine
971 monoxide in this area. Given their relatively fast photolysis, however, CH_3I and CHBr_3 , as well
972 as CH_2Br_2 , may well have roles in the initiation of reactive bromine and iodine formation in this
973 area.

974 Overall, along with other studies, the findings presented here highlight the potentially
975 important role of saline soil and salt lakes in VHOC emission, and call for further research on
976 VHOC emission rates and controlling mechanisms, and implications on stratospheric and
977 tropospheric chemistry.

978 **Data availability.** Data are available upon request from the corresponding author Eran Tas
979 (eran.tas@mail.huji.ac.il).

980

981 **Author contribution:** ET, AG RR and AW designed the experiments. MS, GL and QL carried
982 out the field measurements and DB carried out the sampled air analyses. GL contributed to
983 designing and constructing a special mechanism for the simultaneous lifting and dropping of
984 sampling canisters. Data curation and formal analysis were performed by ET and MS with
985 support from RR. ET and MS prepared the manuscript with contributions from all co-authors.?

986

987 **Competing interests.** The authors declare that they have no conflict of interest.

988

989 **Acknowledgements**

990 This study was supported by the United States–Israel Binational Science Foundation (grant no.
991 2012287). ET holds the Joseph H. and Belle R. Braun Senior Lectureship in Agriculture.

992

993 **References**

- 994 Albers, C. N., Jacobsen, O. S., Flores, E. M. M., and Johnsen, A. R.: Arctic and Subarctic Natural Soils Emit
995 Chloroform and Brominated Analogues by Alkaline Hydrolysis of Trihaloacetyl Compounds, *Environ Sci*
996 *Technol*, 51, 6131-6138, 10.1021/acs.est.7b00144, 2017.
- 997 Alpert, P., Shafir, H., and Issahary, D.: Recent changes in the climate at the dead sea - A preliminary study,
998 *Climatic Change*, 37, 513-537, Doi 10.1023/A:1005330908974, 1997.
- 999 Bondu, S., Cocquempot, B., Deslandes, E., and Morin, P.: Effects of salt and light stress on the release of
1000 volatile halogenated organic compounds by *Solieria chordalis*: a laboratory incubation study, *Botanica*
1001 *Marina*, 51, 485-492, 10.1515/Bot.2008.056, 2008.
- 1002 Breider, F., and Albers, C. N.: Formation mechanisms of trichloromethyl-containing compounds in the
1003 terrestrial environment: A critical review, *Chemosphere*, 119, 145-154,
1004 10.1016/j.chemosphere.2014.05.080, 2015.
- 1005 Brinckmann, S., Engel, A., Bonisch, H., Quack, B., and Atlas, E.: Short-lived brominated hydrocarbons -
1006 observations in the source regions and the tropical tropopause layer, *Atmos Chem Phys*, 12, 1213-1228,
1007 10.5194/acp-12-1213-2012, 2012.
- 1008 Buchalo, A. S., Nevo, E., Wasser, S. P., Oren, A., and Molitoris, H. P.: Fungal life in the extremely
1009 hypersaline water of the Dead Sea: first records, *P Roy Soc B-Biol Sci*, 265, 1461-1465, DOI
1010 10.1098/rspb.1998.0458, 1998.
- 1011 Butler, J. H., King, D. B., Lobert, J. M., Montzka, S. A., Yvon-Lewis, S. A., Hall, B. D., Warwick, N. J., Mondeel,
1012 D. J., Aydin, M., and Elkins, J. W.: Oceanic distributions and emissions of short-lived halocarbons, *Global*
1013 *Biogeochem Cy*, 21, Artn Gb102310.1029/2006gb002732, 2007.

- 1014 Carpenter, L. J., Green, T. J., Mills, G. P., Bauguitte, S., Penkett, S. A., Zanis, P., Schuepbach, E.,
1015 Schmidbauer, N., Monks, P. S., and Zellweger, C.: Oxidized nitrogen and ozone production efficiencies in
1016 the springtime free troposphere over the Alps, *J Geophys Res-Atmos*, 105, 14547-14559,
1017 Doi10.1029/2000jd900002, 2000.
- 1018 Carpenter, L. J., Wevill, D. J., O'Doherty, S., Spain, G., and Simmonds, P. G.: Atmospheric bromoform at
1019 Mace Head, Ireland: seasonality and evidence for a peatland source, *Atmos Chem Phys*, 5, 2927-2934,
1020 DOI 10.5194/acp-5-2927-2005, 2005.
- 1021 Carpenter, L. J., Jones, C. E., Dunk, R. M., Hornsby, K. E., and Woeltjen, J.: Air-sea fluxes of biogenic
1022 bromine from the tropical and North Atlantic Ocean, *Atmos Chem Phys*, 9, 1805-1816, 2009.
- 1023 Carpenter, L. J., MacDonald, S. M., Shaw, M. D., Kumar, R., Saunders, R. W., Parthipan, R., Wilson, J., and
1024 Plane, J. M. C.: Atmospheric iodine levels influenced by sea surface emissions of inorganic iodine,
1025 *Nature Geoscience*, 6, 108-111, 10.1038/Ngeo1687, 2013.
- 1026 Carpenter, L. J., Reimann, S., Burkholder, J. B., Clerbaux, C., Hall, B. D., Hossaini, R., Laube, J. C., and Yvon-
1027 Lewis, S. A.: Ozone-depleting substances (ODSs) and other gases of interest to the Montreal Protocol,
1028 Chapter 1 in *Scientific Assessment of Ozone Depletion: 2014*, Global Ozone Research and Monitoring
1029 Project – Report No. 55, World Meteorological Organization, Geneva, Switzerland, 2014.
- 1030 Colman, J. J., Swanson, A. L., Meinardi, S., Sive, B. C., Blake, D. R., and Rowland, F. S.: Description of the
1031 analysis of a wide range of volatile organic compounds in whole air samples collected during PEM-
1032 Tropics A and B, *Analytical Chemistry*, 73, 3723-3731, DOI 10.1021/ac010027g, 2001.
- 1033 Dearellano, J. V. G., Duynkerke, P. G., and Zeller, K. F.: Atmospheric Surface-Layer Similarity Theory
1034 Applied to Chemically Reactive Species, *J Geophys Res-Atmos*, 100, 1397-1408, Doi 10.1029/94jd02434,
1035 1995.
- 1036 Derendorp, L., Wishkerman, A., Keppler, F., McRoberts, C., Holzinger, R., and Rockmann, T.: Methyl
1037 chloride emissions from halophyte leaf litter: Dependence on temperature and chloride content,
1038 *Chemosphere*, 87, 483-489, 10.1016/j.chemosphere.2011.12.035, 2012.
- 1039 Deventer, M. J., Jiao, Y., Knox, S. H., Anderson, F., Ferner, M. C., Lewis, J. A., and Rhew, R. C.: Ecosystem-
1040 Scale Measurements of Methyl Halide Fluxes From a Brackish Tidal Marsh Invaded With Perennial
1041 Pepperweed (*Lepidium latifolium*), *J Geophys Res-Atmos-Biogeosciences*, 10.1029/2018JG004536,
1042 2018.
- 1043 Dimmer, C. H., Simmonds, P. G., Nickless, G., and Bassford, M. R.: Biogenic fluxes of halomethanes from
1044 Irish peatland ecosystems, *Atmos Environ*, 35, 321-330, Doi 10.1016/S1352-2310(00)00151-5, 2001.
- 1045 Dyer, A. J., and Bradley, E. F.: An Alternative Analysis of Flux-Gradient Relationships at the 1976 Itce,
1046 *Bound-Lay Meteorol*, 22, 3-19, Doi 10.1007/Bf00128053, 1982.
- 1047 Ekdahl, A., Pedersen, M., and Abrahamsson, K.: A study of the diurnal variation of biogenic volatile
1048 halocarbons, *Mar Chem*, 63, 1-8, Doi 10.1016/S0304-4203(98)00047-4, 1998.
- 1049 Gan, J., Yates, S. R., Ohr, H. D., and Sims, J. J.: Production of methyl bromide by terrestrial higher plants,
1050 *Geophys Res Lett*, 25, 3595-3598, Doi 10.1029/98gl52697, 1998.
- 1051 Gebhardt, S., Colomb, A., Hofmann, R., Williams, J., and Lelieveld, J.: Halogenated organic species over the
1052 tropical South American rainforest, *Atmos Chem Phys*, 8, 3185-3197, 2008.
- 1053 Gifford, F. A.: Turbulent diffusion typing schemes: A review," under (R. L. Schoup, Ed.) "Consequences of
1054 Effluent Release, *Nucl. Safety* 17 (I), 6846, 1976. EPA, United States Environmental Protection Agency
1055 Meteorological Monitoring Guidance for Regulatory Modeling Applications, 2000.
- 1056 Golder, D.: Relations among stability parameters in the surface layer ;3(1):47–58., *Boundary-Layer*
1057 *Meteorol*, 31, 47-58, 1972.
- 1058 Grubbs, F. E., and Beck, G.: Extension of Sample Sizes and Percentage Points for Significance Tests of
1059 Outlying Observations, *Technometrics*, 14, 847-&, Doi 10.2307/1267134, 1972.
- 1060 Gualtieri, G., and Secci, S.: Comparing methods to calculate atmospheric stability-dependent wind speed
1061 profiles: A case study on coastal location, *Renew Energ*, 36, 2189-2204, 10.1016/j.renene.2011.01.023,
1062 2011.
- 1063 Hebestreit, K., Stutz, J., Rosen, D., Matveiv, V., Peleg, M., Luria, M., and Platt, U.: DOAS measurements of
1064 tropospheric bromine oxide in mid-latitudes, *Science*, 283, 55-57, DOI 10.1126/science.283.5398.55,
1065 1999.

1066 Hoekstra, E. J., De Leer, E. W. B., and Brinkman, U. A. T.: Natural formation of chloroform and brominated
1067 trihalomethanes in soil, *Environ Sci Technol*, 32, 3724-3729, DOI 10.1021/es980127c, 1998.

1068 Hossaini, R., Chipperfield, M. P., Monge-Sanz, B. M., Richards, N. A. D., Atlas, E., and Blake, D. R.:
1069 Bromoform and dibromomethane in the tropics: a 3-D model study of chemistry and transport, *Atmos*
1070 *Chem Phys*, 10, 719-735, 10.5194/acp-10-719-2010, 2010.

1071 Hossaini, R., Mantle, H., Chipperfield, M. P., Montzka, S. A., Hamer, P., Ziska, E., Quack, B., Kruger, K.,
1072 Tegtmeier, S., Atlas, E., Sala, S., Engel, A., Bonisch, H., Keber, T., Oram, D., Mills, G., Ordonez, C., Saiz-
1073 Lopez, A., Warwick, N., Liang, Q., Feng, W., Moore, E., Miller, B. R., Marecal, V., Richards, N. A. D., Dorf,
1074 M., and Pfeilsticker, K.: Evaluating global emission inventories of biogenic bromocarbons, *Atmos Chem*
1075 *Phys*, 13, 11819-11838, 10.5194/acp-13-11819-2013, 2013.

1076 Huber, S. G., Kotte, K., Scholer, H. F., and Williams, J.: Natural Abiotic Formation of Trihalomethanes in
1077 Soil: Results from Laboratory Studies and Field Samples, *Environ Sci Technol*, 43, 4934-4939,
1078 10.1021/es8032605, 2009.

1079 IPCC (Ed.) Contribution of Working Group I to the Fourth Assessment Report of the Intergovernmental
1080 Panel on Climate Change. , Cambridge University Press, Cambridge, United Kingdom and New York, NY,
1081 USA, 2007.

1082 Jacob, J. H., Hussein, E. I., Shakhathreh, M. A. K., and Cornelison, C. T.: Microbial community analysis of the
1083 hypersaline water of the Dead Sea using high-throughput amplicon sequencing, *Microbiologyopen*, 6,
1084 ARTN e50010.1002/mbo3.500, 2017.

1085 Keppler, F., Eiden, R., Niedan, V., Pracht, J., and Scholer, H. F.: Halocarbons produced by natural oxidation
1086 processes during degradation of organic matter, *Nature*, 403, 298-301, Doi 10.1038/35002055, 2000.

1087 Khan, M. A. H., Whelan, M. E., and Rhew, R. C.: Effects of temperature and soil moisture on methyl halide
1088 and chloroform fluxes from drained peatland pasture soils, *J Environ Monitor*, 14, 241-249,
1089 10.1039/c1em10639b, 2012.

1090 Kis-Papo, T., Grishkan, I., Oren, A., Wasser, S. P., and Nevo, E.: Spatiotemporal diversity of filamentous
1091 fungi in the hypersaline Dead Sea, *Mycol Res*, 105, 749-756, Doi 10.1017/S0953756201004129, 2001.

1092 Kotte, K., Low, F., Huber, S. G., Krause, T., Mulder, I., and Scholer, H. F.: Organohalogen emissions from
1093 saline environments - spatial extrapolation using remote sensing as most promising tool,
1094 *Biogeosciences*, 9, 1225-1235, 10.5194/bg-9-1225-2012, 2012.

1095 Kuyper, B., Palmer, C. J., Labuschagne, C., and Reason, C. J. C.: Atmospheric bromoform at Cape Point,
1096 South Africa: an initial fixed-point data set on the African continent, *Atmos Chem Phys*, 18, 5785-5797,
1097 10.5194/acp-18-5785-2018, 2018.

1098 Lee-Taylor, J. M., and Holland, E. A.: Litter decomposition as a potential natural source of methyl bromide,
1099 *J Geophys Res-Atmos*, 105, 8857-8864, Doi 10.1029/1999jd901112, 2000.

1100 Lenschow, D. H.: Micrometeorological techniques for measuring biosphere-atmosphere trace gas
1101 exchange. *Biogenic Trace Gases: Measuring Emissions from Soil and Water*, P.A. Matson and R.C. Hariss,
1102 Eds., *Methods in Ecology*, Blackwell Science, Oxford, 126-163., 1995.

1103 Liu, Y. N., Yvon-Lewis, S. A., Hu, L., Salisbury, J. E., and O'Hern, J. E.: CHBr₃, CH₂Br₂, and CHClBr₂ in U.S.
1104 coastal waters during the Gulf of Mexico and East Coast Carbon cruise, *J Geophys Res-Oceans*, 116, Artn
1105 C1000410.1029/2010jc006729, 2011.

1106 Maier, M., and Schack-Kirchner, H.: Using the gradient method to determine soil gas flux: A review,
1107 *Agricultural and Forest Meteorology*, 192, 78-95, 10.1016/j.agrformet.2014.03.006, 2014.

1108 Manley, S. L., and Dastoor, M. N.: Methyl-Iodide (CH₃I) Production by Kelp and Associated Microbes,
1109 *Marine Biology*, 98, 477-482, Doi 10.1007/Bf00391538, 1988.

1110 Manley, S. L., Wang, N. Y., Walser, M. L., and Cicerone, R. J.: Coastal salt marshes as global methyl halide
1111 sources from determinations of intrinsic production by marsh plants, *Global Biogeochem Cy*, 20, Artn
1112 Gb301510.1029/2005gb002578, 2006.

1113 Matveev, V., Peleg, M., Rosen, D., Tov-Alper, D. S., Hebestreit, K., Stutz, J., Platt, U., Blake, D., and Luria,
1114 M.: Bromine oxide - ozone interaction over the Dead Sea, *J Geophys Res-Atmos*, 106, 10375-10387, Doi
1115 10.1029/2000jd900611, 2001.

- 1116 Meredith, L. K., Commane, R., Munger, J. W., Dunn, A., Tang, J., Wofsy, S. C., and Prinn, R. G.: Ecosystem
1117 fluxes of hydrogen: a comparison of flux-gradient methods, *Atmospheric Measurement Techniques*, 7,
1118 2787-2805, 10.5194/amt-7-2787-2014, 2014.
- 1119 Moore, R. M., Gut, A., and Andreae, M. O.: A pilot study of methyl chloride emissions from tropical
1120 woodrot fungi, *Chemosphere*, 58, 221-225, 10.1016/j.chemosphere.2004.03.011, 2005.
- 1121 Moore, R. M.: Methyl halide production and loss rates in sea water from field incubation experiments,
1122 *Mar Chem*, 101, 213-219, 10.1016/j.marchem.2006.03.003, 2006.
- 1123 Nadzir, M. S. M., Phang, S. M., Abas, M. R., Rahman, N. A., Abu Samah, A., Sturges, W. T., Oram, D. E.,
1124 Mills, G. P., Leedham, E. C., Pyle, J. A., Harris, N. R. P., Robinson, A. D., Ashfold, M. J., Mead, M. I., Latif,
1125 M. T., Khan, M. F., Amiruddin, A. M., Banan, N., and Hanafiah, M. M.: Bromocarbons in the tropical
1126 coastal and open ocean atmosphere during the 2009 Prime Expedition Scientific Cruise (PESC-09),
1127 *Atmos Chem Phys*, 14, 8137-8148, 10.5194/acp-14-8137-2014, 2014.
- 1128 Niemi, T. M., Ben-Avraham, Z., and Gat, J.R.: *The Dead Sea: The Lake and Its Setting*, Oxford Monogr. Geol.
1129 Geophys. v. ol. 36, Oxford Univ. Press, New York., 1997.
- 1130 O'Brien, L. M., Harris, N. R. P., Robinson, A. D., Gostlow, B., Warwick, N., Yang, X., and Pyle, J. A.:
1131 Bromocarbons in the tropical marine boundary layer at the Cape Verde Observatory - measurements
1132 and modelling, *Atmos Chem Phys*, 9, 9083-9099, 10.5194/acp-9-9083-2009, 2009.
- 1133 O'Dowd, C. D., Jimenez, J. L., Bahreini, R., Flagan, R. C., Seinfeld, J. H., Hameri, K., Pirjola, L., Kulmala, M.,
1134 Jennings, S. G., and Hoffmann, T.: Marine aerosol formation from biogenic iodine emissions, *Nature*,
1135 417, 632-636, DOI 10.1038/nature00775, 2002.
- 1136 Obrist, D., Tas, E., Peleg, M., Matveev, V., Fain, X., Asaf, D., and Luria, M.: Bromine-induced oxidation of
1137 mercury in the mid-latitude atmosphere, *Nature Geoscience*, 4, 22-26, 10.1038/Ngeo1018, 2011.
- 1138 Oren, A., and Shilo, M.: Factors Determining the Development of Algal and Bacterial Blooms in the Dead-
1139 Sea - a Study of Simulation Experiments in Outdoor Ponds, *Fems Microbiol Ecol*, 31, 229-237, 1985.
- 1140 Oren, A., Ionescu, D., Hindiyeh, M., and Malkawi, H.: Microalgae and cyanobacteria of the Dead Sea and
1141 its surrounding springs, *Isr J Plant Sci*, 56, 1-13, Doi 10.1560/Ijps.56.1-2.1, 2008.
- 1142 Osman, K. T.: Forest soils: properties and management. In 'Physical properties of forest soils', 19-28,
1143 2013.
- 1144 Pasquill, F., and Smith, F. B.: The physical and meteorological basis for the estimation of the dispersion of
1145 windborn material, in (H. M. Englund and W. T. Beery, Eds.), *Proceedings of the Second International
1146 Clean Air Congress*, Washington, DC, 1970, pp. 1067-1072, Academic Press, New York, , 1971.
- 1147 Pedersen, M., Collen, J., Abrahamsson, K., and Ekdahl, A.: Production of halocarbons from seaweeds: An
1148 oxidative stress reaction?, *Scientia Marina*, 60, 257-263, 1996.
- 1149 Pen-Mouratov, S., Myblat, T., Shamir, I., Barness, G., and Steinberger, Y.: Soil Biota in the Arava Valley of
1150 Negev Desert, Israel, *Pedosphere*, 20, 273-284, Doi 10.1016/S1002-0160(10)60015-X, 2010.
- 1151 Pyle, J. A., Ashfold, M. J., Harris, N. R. P., Robinson, A. D., Warwick, N. J., Carver, G. D., Gostlow, B.,
1152 O'Brien, L. M., Manning, A. J., Phang, S. M., Yong, S. E., Leong, K. P., Ung, E. H., and Ong, S.: Bromoform
1153 in the tropical boundary layer of the Maritime Continent during OP3, *Atmos Chem Phys*, 11, 529-542,
1154 10.5194/acp-11-529-2011, 2011.
- 1155 Quack, B., and Wallace, D. W. R.: Air-sea flux of bromoform: Controls, rates, and implications (vol 17, art
1156 no 1023, 2003), *Global Biogeochem Cy*, 18, Artn Gb100410.1029/2003gb002187, 2004.
- 1157 Quack, B., Atlas, E., Petrick, G., and Wallace, D. W. R.: Bromoform and dibromomethane above the
1158 Mauritanian upwelling: Atmospheric distributions and oceanic emissions, *J Geophys Res-Atmos*, 112,
1159 Artn D0931210.1029/2006jd007614, 2007.
- 1160 Rhew, R. C., Miller, B. R., and Weiss, R. F.: Natural methyl bromide and methyl chloride emissions from
1161 coastal salt marshes, *Nature*, 403, 292-295, Doi 10.1038/35002043, 2000.
- 1162 Rhew, R. C., Miller, B. R., Vollmer, M. K., and Weiss, R. F.: Shrubland fluxes of methyl bromide and methyl
1163 chloride, *J Geophys Res-Atmos*, 106, 20875-20882, Doi 10.1029/2001jd000413, 2001.
- 1164 Rhew, R. C., Miller, B. R., Bill, M., Goldstein, A. H., and Weiss, R. F.: Environmental and biological controls
1165 on methyl halide emissions from southern California coastal salt marshes, *Biogeochemistry*, 60, 141-
1166 161, Doi 10.1023/A:1019812006560, 2002.

- 1167 Rhew, R. C., Aydin, M., and Saltzman, E. S.: Measuring terrestrial fluxes of methyl chloride and methyl
1168 bromide using a stable isotope tracer technique, *Geophys Res Lett*, 30, Artn
1169 210310.1029/2003gl018160, 2003.
- 1170 Rhew, R. C., Teh, Y. A., Abel, T., Atwood, A., and Mazeas, O.: Chloroform emissions from the Alaskan Arctic
1171 tundra, *Geophys Res Lett*, 35, Artn L2181110.1029/2008gl035762, 2008.
- 1172 Rhew, R. C., Whelan, M. E., and Min, D. H.: Large methyl halide emissions from south Texas salt marshes,
1173 *Biogeosciences*, 11, 6427-6434, 10.5194/bg-11-6427-2014, 2014.
- 1174 Rousseaux, M. C., Ballare, C. L., Giordano, C. V., Scopel, A. L., Zima, A. M., Szwarcberg-Bracchitta, M.,
1175 Searles, P. S., Caldwell, M. M., and Diaz, S. B.: Ozone depletion and UVB radiation: Impact on plant DNA
1176 damage in southern South America, *Proceedings of the National Academy of Sciences of the United
1177 States of America*, 96, 15310-15315, DOI 10.1073/pnas.96.26.15310, 1999.
- 1178 Ruecker, A., Weigold, P., Behrens, S., Jochmann, M., Laaks, J., and Kappler, A.: Predominance of Biotic over
1179 Abiotic Formation of Halogenated Hydrocarbons in Hypersaline Sediments in Western Australia,
1180 *Environ Sci Technol*, 48, 9170-9178, 10.1021/es501810g, 2014.
- 1181 Schmutge, T. J., and André, J.-C.: Land surface evaporation: measurement and parameterization: Springer
1182 Science & Business Media, 1991.
- 1183 Simmonds, P. G., Derwent, R. G., Manning, A. J., O'Doherty, S., and Spain, G.: Natural chloroform
1184 emissions from the blanket peat bogs in the vicinity of Mace Head, Ireland over a 14-year period, *Atmos
1185 Environ*, 44, 1284-1291, 10.1016/j.atmosenv.2009.12.027, 2010.
- 1186 Simpson, W. R., Brown, S. S., Saiz-Lopez, A., Thornton, J. A., and von Glasow, R.: Tropospheric Halogen
1187 Chemistry: Sources, Cycling, and Impacts, *Chemical Reviews*, 115, 4035-4062, 10.1021/cr5006638,
1188 2015.
- 1189 Sive, B. C., Varner, R. K., Mao, H., Blake, D. R., Wingenter, O. W., and Talbot, R.: A large terrestrial source
1190 of methyl iodide, *Geophys Res Lett*, 34, Artn L1780810.1029/2007gl030528, 2007.
- 1191 Stull, R. B.: An introduction to boundary layer meteorology. Kluwer, Dordrecht1988.
- 1192 Sverdrup, H. U., Johnson, M.W., and Fleming, R.H.: The Oceans, Their Physics, Chemistry and General
1193 Biology, Prentice-Hall, Englewood Cliffs, N.J., 1942.
- 1194 Tas, E., Matveev, V., Zingler, J., Luria, M., and Peleg, M.: Frequency and extent of ozone destruction
1195 episodes over the Dead Sea, Israel, *Atmos Environ*, 37, 4769-4780, 10.1016/j.atmosenv.2003.08.015,
1196 2003.
- 1197 Tas, E., Peleg, M., Matveev, V., Zingler, J., and Luria, M.: Frequency and extent of bromine oxide formation
1198 over the Dead Sea, *J Geophys Res-Atmos*, 110, Artn D1130410.1029/2004jd005665, 2005.
- 1199 Tas, E., Peleg, M., Pedersen, D. U., Matveev, V., Biazar, A. P., and Luria, M.: Measurement-based modeling
1200 of bromine chemistry in the boundary layer: 1. Bromine chemistry at the Dead Sea, *Atmos Chem Phys*,
1201 6, 5589-5604, 2006.
- 1202 Tas, E., Obrist, D., Peleg, M., Matveev, V., Fain, X., Asaf, D., and Luria, M.: Measurement-based modelling
1203 of bromine-induced oxidation of mercury above the Dead Sea, *Atmos Chem Phys*, 12, 2429-2440,
1204 10.5194/acp-12-2429-2012, 2012.
- 1205 Varner, R. K., Crill, P. M., and Talbot, R. W.: Wetlands: a potentially significant source of atmospheric
1206 methyl bromide and methyl chloride, *Geophys Res Lett*, 26, 2433-2435, Doi 10.1029/1999gl0900587,
1207 1999.
- 1208 Warwick, N. J., Pyle, J. A., and Shallcross, D. E.: Global modelling of the atmospheric methyl bromide
1209 budget, *J Atmos Chem*, 54, 133-159, 10.1007/s10874-006-9020-3, 2006.
- 1210 Watling, R., and Harper, D. B.: Chloromethane production by wood-rotting fungi and an estimate of the
1211 global flux to the atmosphere, *Mycol Res*, 102, 769-787, Doi 10.1017/S0953756298006157, 1998.
- 1212 Weissflog, L., Lange, C. A., Pfennigsdorff, A., Kotte, K., Elansky, N., Lisitzyna, L., Putz, E., and Krueger, G.:
1213 Sediments of salt lakes as a new source of volatile highly chlorinated C1/C2 hydrocarbons, *Geophys Res
1214 Lett*, 32, Artn L0140110.1029/2004gl020807, 2005.

1215 Wishkerman, A., Gebhardt, S., McRoberts, C. W., Hamilton, J. T. G., Williams, J., and Keppler, F.: Abiotic
1216 methyl bromide formation from vegetation, and its strong dependence on temperature, *Environ Sci*
1217 *Technol*, 42, 6837-6842, 10.1021/es800411j, 2008.

1218 WMO, W. M. O.: *Guide to Meteorological Instruments and Methods of Observation*, 2008.

1219 Xiao, X., Prinn, R. G., Fraser, P. J., Simmonds, P. G., Weiss, R. F., O'Doherty, S., Miller, B. R., Salameh, P. K.,
1220 Harth, C. M., Krummel, P. B., Porter, L. W., Muhle, J., Grealley, B. R., Cunnold, D., Wang, R., Montzka, S.
1221 A., Elkins, J. W., Dutton, G. S., Thompson, T. M., Butler, J. H., Hall, B. D., Reimann, S., Vollmer, M. K.,
1222 Stordal, F., Lunder, C., Maione, M., Arduini, J., and Yokouchi, Y.: Optimal estimation of the surface fluxes
1223 of methyl chloride using a 3-D global chemical transport model, *Atmos Chem Phys*, 10, 5515-5533,
1224 10.5194/acp-10-5515-2010, 2010.

1225 Yang, K., Tamai, N., and Koike, T.: Analytical solution of surface layer similarity equations, *J Appl Meteorol*,
1226 40, 1647-1653, Doi 10.1175/1520-0450(2001)040<1647:Asosls>2.0.Co;2, 2001.

1227 Yassaa, N., Wishkerman, A., Keppler, F., and Williams, J.: Fast determination of methyl chloride and methyl
1228 bromide emissions from dried plant matter and soil samples using HS-SPME and GC-MS: method and
1229 first results, *Environmental Chemistry*, 6, 311-318, 10.1071/En09034, 2009.

1230 Yokouchi, Y., Ikeda, M., Inuzuka, Y., and Yukawa, T.: Strong emission of methyl chloride from tropical
1231 plants, *Nature*, 416, 163-165, DOI 10.1038/416163a, 2002.

1232 Yokouchi, Y., Inagaki, T., Yazawa, K., Tamaru, T., Enomoto, T., and Izumi, K.: Estimates of ratios of
1233 anthropogenic halocarbon emissions from Japan based on aircraft monitoring over Sagami Bay, Japan, *J*
1234 *Geophys Res-Atmos*, 110, Artn D0630110.1029/2004jd005320, 2005.

1235 Yokouchi, Y., Saito, T., Ishigaki, C., and Aramoto, M.: Identification of methyl chloride-emitting plants and
1236 atmospheric measurements on a subtropical island, *Chemosphere*, 69, 549-553,
1237 10.1016/j.chemosphere.2007.03.028, 2007.

1238 Zhou, Y., Varner, R. K., Russo, R. S., Wingenter, O. W., Haase, K. B., Talbot, R., and Sive, B. C.: Coastal water
1239 source of short-lived halocarbons in New England, *J Geophys Res-Atmos*, 110, Artn
1240 D2130210.1029/2004jd005603, 2005.

1241 Zhou, Y., Mao, H. T., Russo, R. S., Blake, D. R., Wingenter, O. W., Haase, K. B., Ambrose, J., Varner, R. K.,
1242 Talbot, R., and Sive, B. C.: Bromoform and dibromomethane measurements in the seacoast region of
1243 New Hampshire, 2002-2004, *J Geophys Res-Atmos*, 113, Artn D0830510.1029/2007jd009103, 2008.

1244 Zingler, J., and Platt, U.: Iodine oxide in the Dead Sea Valley: Evidence for inorganic sources of boundary
1245 layer IO, *J Geophys Res-Atmos*, 110, Artn D0730710.1029/2004jd004993, 2005.

1246 Ziska, F., Quack, B., Abrahamsson, K., Archer, S. D., Atlas, E., Bell, T., Butler, J. H., Carpenter, L. J., Jones, C.
1247 E., Harris, N. R. P., Hepach, H., Heumann, K. G., Hughes, C., Kuss, J., Kruger, K., Liss, P., Moore, R. M.,
1248 Orlikowska, A., Raimund, S., Reeves, C. E., Reifenhauer, W., Robinson, A. D., Schall, C., Tanhua, T.,
1249 Tegtmeier, S., Turner, S., Wang, L., Wallace, D., Williams, J., Yamamoto, H., Yvon-Lewis, S., and
1250 Yokouchi, Y.: Global sea-to-air flux climatology for bromoform, dibromomethane and methyl iodide,
1251 *Atmos Chem Phys*, 13, 8915-8934, 10.5194/acp-13-8915-2013, 2013.

1252